ISSN 2531-2960

Volume 4, Issue 14 — July — December - 2020

Journal of Technological Development

ECORFAN®

Journal of Technological Development
Volume 4, Issue 14, July – December 2020, is a journal edited sixmonthly by ECORFAN. 38 Matacerquillas street, Postcode: 28411. Moralzarzal – Madrid WEB: www.ecorfan.org/spain, journal@ecorfan.org. Editor in Chief: BANERJEE, Bidisha. PhD, ISSN On line: 2531-2960. Responsible for the latest update of this number ECORFAN Computer Unit. ESCAMILLA-BOUCHÁN, Imelda. PhD, LUNA-SOTO, Vladimir. PhD, 38 Matacerquillas street, Postcode: 28411. Moralzarzal – Madrid, last updated December 31, 2020.

Journal of Technological Development

Definition of Research Journal

Scientific Objectives

Support the international scientific community in its written production Science, Technology and Innovation in the Field of Engineering and Technology in Subdisciplines of technological development, digital technology, technological impact, teaching with computer help, reliability of computers, heuristics, computing, machine arithmetic instructions, artificial intelligence, algorithmic languages, programming languages

ECORFAN-Mexico SC is a Scientific and Technological Company in contribution to the Human Resource training focused on the continuity in the critical analysis of International Research and is attached to CONACYT-RENIECYT number 1702902, its commitment is to disseminate research and contributions of the International Scientific Community, academic institutions, agencies and entities of the public and private sectors and contribute to the linking of researchers who carry out scientific activities, technological developments and training of specialized human resources with governments, companies and social organizations.

Encourage the interlocution of the International Scientific Community with other Study Centers in Mexico and abroad and promote a wide incorporation of academics, specialists and researchers to the publication in Science Structures of Autonomous Universities - State Public Universities - Federal IES - Polytechnic Universities - Technological Universities - Federal Technological Institutes - Normal Schools - Decentralized Technological Institutes - Intercultural Universities - S & T Councils - CONACYT Research Centers.

Scope, Coverage and Audience

Journal of Technological Development is a Research Journal edited by ECORFAN-Mexico S.C in its Holding with repository in Spain, is a scientific publication arbitrated and indexed with semester periods. It supports a wide range of contents that are evaluated by academic peers by the Double-Blind method, around subjects related to the theory and practice of technological development, digital technology, technological impact, teaching with computer help, reliability of computers, heuristics, computing, machine arithmetic instructions, artificial intelligence, algorithmic languages, programming languages with diverse approaches and perspectives, that contribute to the diffusion of the development of Science Technology and Innovation that allow the arguments related to the decision making and influence in the formulation of international policies in the Field of Engineering and Technology. The editorial horizon of ECORFAN-Mexico® extends beyond the academy and integrates other segments of research and analysis outside the scope, as long as they meet the requirements of rigorous argumentative and scientific, as well as addressing issues of general and current interest of the International Scientific Society.

Editorial Board

Arbitration Committee

Assignment of Rights

The sending of an Article to Journal of Technological Development emanates the commitment of the author not to submit it simultaneously to the consideration of other series publications for it must complement the Originality Format for its Article.

The authors sign the Authorization Format for their Article to be disseminated by means that ECORFAN-Mexico, S.C. In its Holding Spain considers pertinent for disclosure and diffusion of its Article its Rights of Work.

Declaration of Authorship

Indicate the Name of Author and Coauthors at most in the participation of the Article and indicate in extensive the Institutional Affiliation indicating the Department.

Identify the Name of Author and Coauthors at most with the CVU Scholarship Number-PNPC or SNI-CONACYT- Indicating the Researcher Level and their Google Scholar Profile to verify their Citation Level and H index.

Identify the Name of Author and Coauthors at most in the Science and Technology Profiles widely accepted by the International Scientific Community ORC ID - Researcher ID Thomson - arXiv Author ID - PubMed Author ID - Open ID respectively.

Indicate the contact for correspondence to the Author (Mail and Telephone) and indicate the Researcher who contributes as the first Author of the Article.

Plagiarism Detection

All Articles will be tested by plagiarism software PLAGSCAN if a plagiarism level is detected Positive will not be sent to arbitration and will be rescinded of the reception of the Article notifying the Authors responsible, claiming that academic plagiarism is criminalized in the Penal Code.

Arbitration Process

All Articles will be evaluated by academic peers by the Double Blind method, the Arbitration Approval is a requirement for the Editorial Board to make a final decision that will be final in all cases. MARVID® is a derivative brand of ECORFAN® specialized in providing the expert evaluators all of them with Doctorate degree and distinction of International Researchers in the respective Councils of Science and Technology the counterpart of CONACYT for the chapters of America-Europe-Asia- Africa and Oceania. The identification of the authorship should only appear on a first removable page, in order to ensure that the Arbitration process is anonymous and covers the following stages: Identification of the Research Journal with its author occupation rate - Identification of Authors and Coauthors - Detection of plagiarism PLAGSCAN - Review of Formats of Authorization and Originality-Allocation to the Editorial Board- Allocation of the pair of Expert Arbitrators-Notification of Arbitration -Declaration of observations to the Author-Verification of Article Modified for Editing-Publication.

Instructions for Scientific, Technological and Innovation Publication

Knowledge Area

The works must be unpublished and refer to topics of technological development, digital technology, technological impact, teaching with computer help, reliability of computers, heuristics, computing, machine arithmetic instructions, artificial intelligence, algorithmic languages, programming languages and other topics related to Engineering and Technology.

Presentation of the Content

In the first chapter we present, *Increased intensity of interference fringes in Digital Holography, by LÓPEZ-ÁLVAREZ, Yadira Fabiola*, PEÑA-LECONA, Francisco Gerardo, JARA-RUIZ, Ricardo and HERRERA-SERRANO, Jorge Eduardo, with ascription in the Universidad Tecnológica del Norte de Aguascalientes and Universidad de Guadalajara, as a second article we present, *Exergy analysis of the absorption refrigeration cycle using economizers*, by VALENCIA-ALEJANDRO, Eric A., HERRERA-ROMERO, José V., COLORADO-GARRIDO, Darío and SILVA-AGUILAR, Oscar F., with ascription in the Universidad Veracruzana, as the following article we present, *Mathematical modeling of the diffusion of liquids in the gaseous phase by evaporation*, by LOPEZ-VALDIVIESO, Leticia, ELISEO-DANTÉS, Hortensia, CASTRO-DE LA CRUZ, Jucelly and TEJERO-RIVAS, María Candelaria, with ascription in the Instituto Tecnológico de Villahermosa, as the following article we present, *Turbidity, dissolved Oxygen and pH measurement system for grey water treatment process by electrocoagulation*, by CANTERA-CANTERA, Luis Alberto, CALVILLO-TÉLLEZ, Andrés and LOZANO-HERNANDEZ, Yair, with ascription in the Instituto Politécnico Nacional.

Contet

Artícle **Journal of Technological Development**
December, 2020 Vol.4 No.14 1-6

Increased intensity of interference fringes in Digital Holography

Aumento de la intensidad de franjas de interferencia en Holografía Digital

LÓPEZ-ÁLVAREZ, Yadira Fabiola[1,2]†*, PEÑA-LECONA, Francisco Gerardo[2], JARA-RUIZ, Ricardo[1] and HERRERA-SERRANO, Jorge Eduardo[1]

[1]*Universidad Tecnológica del Norte de Aguascalientes, Estación Rincón, Rincón de Romos, Aguascalientes, 20400 México.*
[2]*Departamento de Ciencias Exactas y Tecnología, Centro Universitario de los Lagos, CULagos. Universidad de Guadalajara, Lagos de Moreno, Jalisco, 47460, México*

ID 1st Author: *Yadira Fabiola, López-Álvarez* / **ORC ID**: 0000-0002-9041-1908, **Researcher ID Thomson**: T-1555-2018, **CVU CONACYT ID**: 375952

ID 1st Coauthor: *Francisco Gerardo, Peña-Lecona* / **ORC ID**: 0000-0002-9537-8633, **CVU CONACYT ID**: 122563

ID 2nd Coauthor: *Ricardo, Jara-Ruiz* / **ORC ID**: 0000-0001-7725-4138, **Researcher ID Thomson**: T-1532-2018, **CVU CONACYT ID**: 630276

ID 3rd Coauthor: *Jorge Eduardo, Herrera-Serrano* / **ORC ID**: 0000-0002-3960-8406, **CVU CONACYT ID**: 881987

DOI: 10.35429/JTD.2019.12.3.1.6 Received June 26, 2020; Accepted November 28, 2020

Abstract

Digital holographic interferometry is a full field optical technique, used in the measurement of dynamic and non-contact events, this technique works with arrays where the initial acquisition of interference fringes is not necessary, but rather involves the superposition of two wave fronts. Where from the holograms and by means of a Fourier window-based processing it is feasible to recover the information of both intensity and phase. However, the interference fringes resulting from the demodulation of the holograms may have low intensity, affecting their subsequent analysis. In this work, the combination of the holographic techniques, filters and the superposition principle is proposed to increase the intensity of the fringes, the results show that using the Fourier method in combination with the superposition theorem is possible to obtain greater intensity between the minimum and maximum of the fringes.

Digital holographic interferometry, Fourier, Filters

Resumen

La interferometría holográfica digital es una técnica óptica de campo completo, utilizada en la medición de eventos dinámicos y de no contacto, esta técnica trabaja con arreglos donde no es necesario la adquisición inicial de franjas de interferencia, si no que implica la superposición de dos frentes de onda, donde a partir de los hologramas y mediante un procesamiento a base de ventanas de Fourier es factible recuperar la información tanto de intensidad como de la fase. Sin embargo, las franjas de interferencia resultantes de la demodulación de los hologramas pueden tener poca intensidad viéndose afectado su posterior análisis. En este trabajo se propone la combinación de técnicas holográficas, filtros y el principio de superposición para aumentar la intensidad de las franjas, los resultados muestran que utilizado el método de Fourier cotidiano en combinación con el teorema de superposición es posible obtener mayor intensidad entre los mínimos y máximos de las franjas.

Interferometría holográfica digital, Fourier, Filtro

Citation: LÓPEZ-ÁLVAREZ, Yadira Fabiola, PEÑA-LECONA, Francisco Gerardo, JARA-RUIZ, Ricardo and HERRERA-SERRANO, Jorge Eduardo. Increased intensity of interference fringes in Digital Holography. Journal of Technological Development. 2020. 4-14: 1-6

* Correspondence to Author (email: beatrizeugenia_m_mtz@yahoo.com.mx)
† Researcher contributing first author.

Introduction

The development of systems for the measurement of physical variables has applications in different industrial areas such as automotive, naval, aerospace, biochemistry, and even medicine (Huggins, 1992), (Aguado, 2017), (X.J., 2003).Technological advances require that these devices present design and operation advantages over every day industrial instrumentation (Giallorenzi, 1982), so the incorporation of devices with micro-scale technology would meet the size and accessibility requirements, however, these imply a complicated construction and design process (Chikovani, 2017).

The use of optical metrology for the monitoring of different variables has had a great boom in recent decades, among the optical techniques highlighting the phase recovery of two wave fronts through cross-correlation techniques (Percival, 2009), (Yamaguchi, 1989), diffraction and polarization (Marciel, 1995). The first devices that make use of fiber optics as a transducer system are based on the Sagnac effect (Kurzych, 2016), Fabry-Perot and Mach-Zehnder (Lutang, 2017), among other configurations, however, their construction requires great stability in the system.

Digital holographic interferometry (DHI), is a non-destructive, full-field optical technique that is used in the measurement of dynamic and static events, it is based on the superposition of two wave fronts, but unlike an interferometer it requires a correlation of two holograms to determine the phase.

In addition to the accessibility of the technique, another advantage that digital holography presents over interferometry is that it can work on rough surfaces, its design is relatively simple and applicable to longitudinal measurements (Saito, 1971). However, in the process of demodulation of holograms, the information contained in them can be affected by noise originated by the same measuring instruments, lenses, mirrors and sensor of the CCD camera (Charge Coupled Device). In this work, a technique to increase the intensity of the interference fringes caused by the correlation of two holograms is presented by superimposing the same signals.

In section 2, the optical system to obtain holograms, in section 3, the numerical principles, the phase estimation, the relationship between a phase difference between two holograms, the interference fringes and the superposition method are shown for greater intensity. In section 4, an experimental example is developed, and the results are shown, and finally in section 5 the conclusions of the work.

Experimental setup

Figure 1 shows the standard optical system, used to obtain holograms in the measurement of different variables, it is applied to measure concentration of liquid substances, temperature changes, among many others.

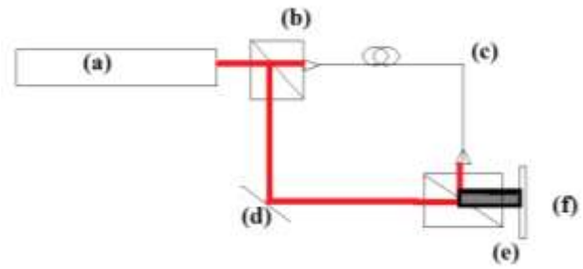

Figure 1 Diagram of the optical system used in DHI, (a) He-Ne 633nm laser, (b) Beam splitter cube 1, (c) Optical fiber, (d) Mirror, (e) Beam splitter cube 2 and (f) CCD camera
Source: Own Elaboration

Methods and development

Digital Holographic Interferometry is a widely studied non-contact optical technique that works with arrangements where the initial acquisition of interference fringes is not necessary, it only involves the superposition of two wave fronts, where from the holograms obtained and by means of in a Fourier window-based processing, it is feasible to recover the information of both the intensity and the phase of the wave fronts from the same source (Kreis, 2005). The intensity detected by the CCD sensor of each image is $I_H(x,y)$, according to equation (1).

$$I_H(x,y) = |U_R(x,y)|^2 + |U_0(x,y)|^2 + U_R^*(x,y)U_0(x,y) + U_R(x,y)U_0^*(x,y) \quad (1)$$

$$U_R(x,y) = u_r(x,y)\exp^{i\varphi(x,y)}$$
$$U_0(x,y) = u_0(x,y)\exp^{-i2\pi(\varphi_x x + \varphi_y y)} = u_0(x,y)\exp^{-i\varphi_1(x,y)} \quad (2)$$

$U_R(x,y)$ and $U_0(x,y)$ are the reference beam and the one passing through the object, (x,y) denote the coordinates in the plane of the hologram, $(\varphi_x x, \varphi_y y)$ describe the spatial frequencies and * denotes the complex conjugate,

Which results in:

$$I_H(x,y) = a(x,y) + c(x,y)e^{i2\pi(\varphi_x x,+\varphi_y y)} + c^*(x,y)e^{-i2\pi(\varphi_x x+ \varphi_y y)} \quad (3)$$

Where:

$$(x,y) = u_r(x,y)^2 + u_0(x,y)^2 \qquad y$$
$$c(x,y) = u_r(x,y) + u_0(x,y)\exp^{i\varphi(x,y)} \quad (4)$$

Applying the Fourier Transform:

$$F\{I_H(x,y)\} = I(u,v) = A(u,v) + C(u - f_x, v - f_y) + C^*(u + f_x, v - f_y) \quad (5)$$

A band-based filter is applied separating one of the last two terms of equation (5), finally obtaining the phase distribution.

$$\varphi(x,y) + 2\pi(f_x x + f_y y) = \arctan\frac{Im[C(u-f_x,v-f_y)]}{Re[C(u-f_x,v-f_y)]} \quad (6)$$

1.1 Determination of phase with DHI.

To determine the phase changes, it is necessary to capture a second hologram determined by:

$$I'_H(x,y) = |U_R(x,y)|^2 + |U'_O(x,y)|^2 + U^*_R(x,y)U'_O(x,y) + U_R(x,y)U'^*_O(x,y) \quad (7)$$

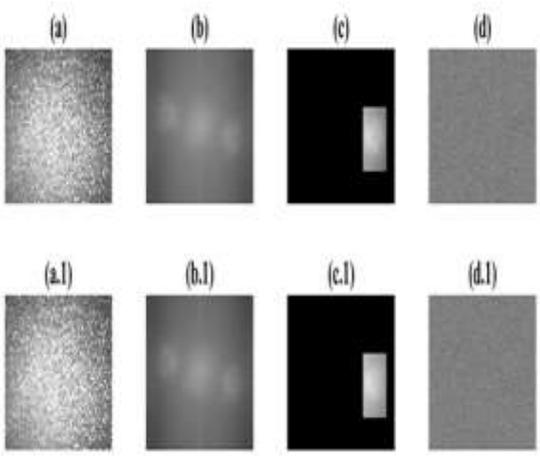

Figure 2 Interference phase recovery process using DHI, *Source: Own Elaboration*

The Figure 2 describes the process of recovery of the phase of two holograms with different states, the deformation was induced in the fiber optic arm shown in Figure 1, (a) $I_H(x,y)$,(a.1) $I'_H(x,y)$, (b) $F\{I_H(x,y)\}$, (b.1) $F\{I'_H(x,y)\}$, (c) $C(u - f_x, v - f_y)$, (c.1) $C'(u - f_x, v - f_y)$, (d) $\varphi(x,y) + 2\pi(f_x x + f_y y)$ y (d.1) $\varphi'_1(x,y) + 2\pi(f_x x + f_y y)$, to obtain a phase difference between the two states, the reference state and the one that undergoes an optical path change, it is considered that the reference remains constant in the experiment, $U_R(x,y) = u_r(x,y)\exp^{i\varphi(x,y)}$, while the beam passing through the optical fiber will exhibit a phase shift, $U'_O(x,y) = u'_0(x,y)\exp^{i\varphi'_1(x,y)}$.

Diferencia de fase entre dos hologramas

The pattern of interference fringes that is characteristic between two states can be calculated as a subtraction of two phases.

$$\Delta\phi_m = \varphi'_1(x,y) - \varphi(x,y) \quad (8)$$

For the study of dynamic events using DHI, the process involves determining the phase changes at each point of the induced deformation, $\varphi'_j(x,y)$.

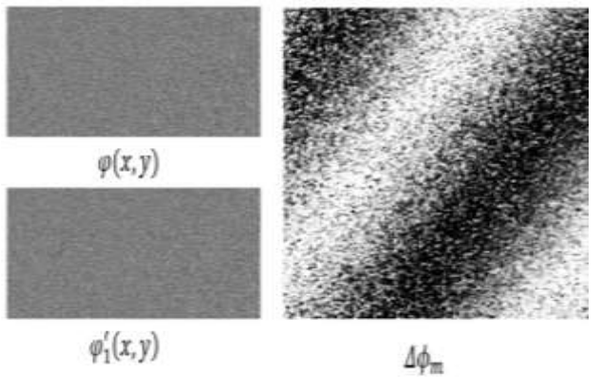

Figure 3 Phase difference between $I_H(x,y)$ and $I'_H(x,y)$ *Source: Own Elaboration*

Method of enhancing fringes by superposition

In the region where the waves are superimposed, the intensity varies between one point and another of each of the signals, obtaining minimums and maximums, giving rise to constructive or destructive interferences and given that the principle of superposition suggests in general that when two or more waves coincide in time and space, the resulting in a function is the vector sum of the individual wave functions (Buerbano, 2003).

From the wave superposition theorem at a point and considering that the resulting equation must also comply with the wave equation, an approximation can be made in the behavior of the interference fringes with this principle.

Given the:

$$\varphi_1(x,t) = f_1(x+ct) \quad (9)$$

$$\varphi_2(x,t) = f_2(x-ct) \quad (10)$$

$$\varphi_T(x,t) = \varphi_1(x,t) + \varphi_2(x,t) \quad (11)$$

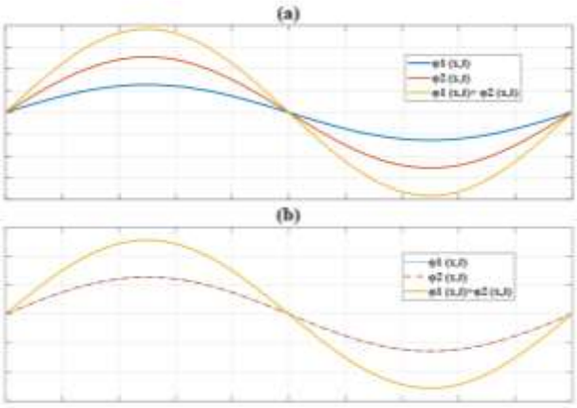

Figure 4 Principle of superposition of two functions, (a) with different amplitude $\varphi_1(x,t) \neq \varphi_2(x,t)$, (b) with equal amplitude $\varphi_1(x,t) = \varphi_2(x,t)$
Source: Own Elaboration

Figure 4 shows two examples of the behavior of the superposition principle used in this work, in (a) the increase in the amplitude of the signal is shown with the algebraic sum of two signals with different amplitude, while in (b) the F1 and F2 signals have the same amplitude.

Fringes pattern demodulation

To determine the phase distribution, PSI phase shift interferometry is a phase map unfolding technique, where it records a series of interferograms with phase differences, as shown by equation (12). To carry out the phase reconstruction process, in general, algorithms with a combination of interferograms are applied; the analysis can be done with $n = 1,2,..M$ interferograms (Schwider, 1983).

$$\tan\varphi = \frac{\sum_{n=1}^{M} b_n I_n}{\sum_{n=1}^{M} a_n I_n} \quad (12)$$

With a_n and b_n, as real coefficients.

Results

For the analysis of the fringes resulting from the phase difference between each hologram, its profile is considered, see Figure 5.

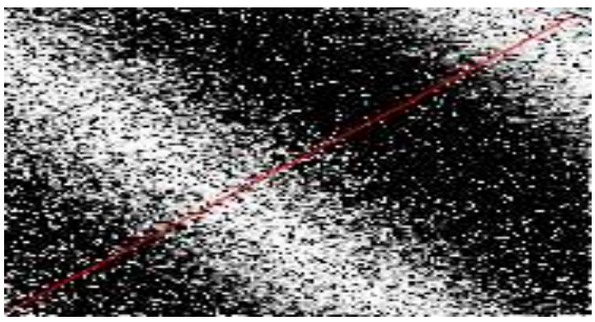

Figure 5 Interference fringes originating from the phase difference of two holograms
Source: Own Elaboration

Figure 6 shows the maximums and minimums of the interference signal, a polynomial approximation is carried out to eliminate noise in the signal. The approximation is used to implement the superposition theorem and show that the amplitude in the intensity of the fringes also increases.

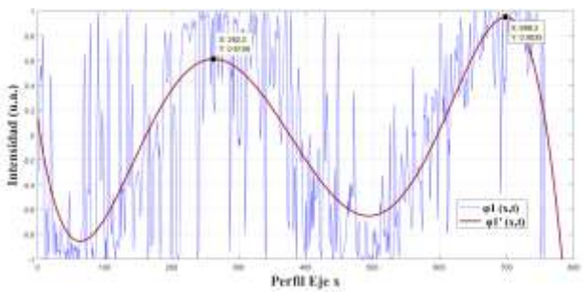

Figure 6 Profile of interference fringes originating from the phase difference of two holograms, with polynomial approximation
Source: Own Elaboration

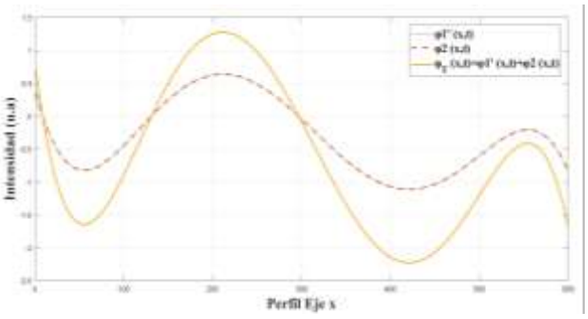

Figure 7 Profile of interference fringes originating from the phase difference of two holograms, with polynomial approximation
Source: Own Elaboration

Figure 7 shows the profile of the interference fringes that were used to increase the intensity in the interference fringes when $\varphi_1(x,t) = \varphi_2(x,t)$.

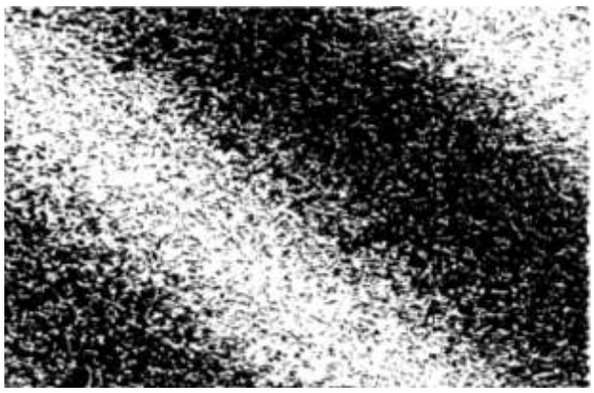

Figure 8 Interference fringes originating from the phase difference of two holograms with twice their intensity
Source: Own Elaboration

Equation (12) is used to determine the characteristic phase map of the interference fringes. In Figure 9 the phase maps for the original interference patterns are shown and when their intensity is increased, the properties are still preserved, which suggests that it is feasible to increase the sharpness of the interference patterns without altering their behavior.

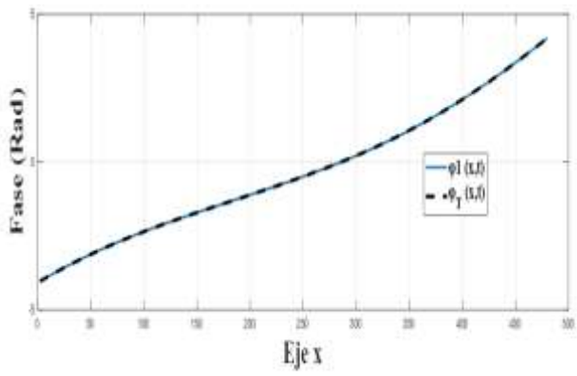

Figure 9 Phase maps of the interference fringes
Source: Own Elaboration

Conclusion

A simple method is presented for increasing the intensity of interference fringes obtained Holographic Interferometry by Digital, the process shows the geometric distribution of the interference fringes is not lost and it continues to retain its same phase map. The proposed intensity increase method is implemented in the difference of holograms with high frequency, where the quality of the fringes is affected, both by the instruments and by the characteristics of the same technique.

References

Aguado Rojas Missie, Pasillas Lépine William, Loría Antonio, De Bernardinis Alexandre. (2017). Angular velocity estimation from incremental encoder measurements incremental encoder measurements in the presence of sensor imperfections. *IFAC-PapersOnLine*.50(1) 5979-5984.

Buerbano Santiago. (2003). Física general, Tébar, SL.

Chikovani, V. V., & Tsiruk, H. V. (2017). Digital rate MEMS vibratory gyroscope modeling, tuning and simulation results. *Computación y Sistemas*, 21(1), 147–159.

Giallorenzi, T. G., Bucaro, J. A., Dandridge, A., Sigel, G. H., Cole, J. H., Rashleigh, S. C., & Priest, R. G. (1982). Optical Fiber Sensor Technology. *IEEE Journal of Quantum Electronics*, 18(4), 626–665.

Huggins, R. W., Abbas, G. L., Hong, C. S., Miller, G. E., Porter, C. R., & Van Deventer, B. (1992). Fiber-coupled position sensors for aerospace applications. *Optics and Lasers in Engineering*, 16(2–3), 79–103.

Kreis, T. (2005). Handbook of holographic interferometry: Optical and Digital Methods. Klagenfurter: WILEY-VCH Verlag GmbH & Co.KGaA.

Kurzych, A., Kowalski, J. K., Sakowicz, B., Krajewski, Z., & Jaroszewicz, L. R. (2016). The laboratory investigation of the innovative sensor for torsional effects in engineering structures' monitoring. *Opto-Electronics Review*.

Lutang Wang and Nian Fang. (2017). Applications of Fiber-Optic Interferometry Technology in Sensor Fields, *InTechOpen*.

Mancier Nathalie, Chakari Ayoub, Meyrueis Patrick, and Clément Michel. (1995). Angular displacement fiber-optic sensor: theoretical and experimental study. *Appl. Opt*., 34(28).

Percival F. Almoro, Giancarlo Pedrini, Arun Anand, Wolfgang Osten, and Steen G. Hanson. (2009). Angular displacement and deformation analyses using a speckle-based wavefront sensor. *Appl. Opt*. 48(5).

ISSN 2531-2960

Saito, H., Yamaguchi, I., & Nakajima, T. (1971). Application of Holographic Interferometry to Mechanical Experiments. *In Applications of Holography*. Springer US, 105-126.

Schwider J., Burow R., Elssner K.-E., Grzanna J., Spolaczyk R., and Merkel K. (1983)."Digital wave-front measuring interferometry: some systematic error sources," *Appl. Opt*. 22, 3421-3432.

X.J. Zhang, S. Rappel, R.W. Bernstein, C.-C. Chenl, 0. Sahin, M. Scott and 0. Solgaard. (October,2003). High-precision characterization of embryo positioning force using mems optical encoder. *7th international Conference on Miniaturized Chemical and Biochemical Analysts Systems*, Squaw Valley, California USA.

Yamaguchi, I. (1989). Encoder and strain gauge using laser speckle. *Optics and Lasers in Engineering*. 11(4), 223–232.

ISSN 2531-2960

Artícle **Journal of Technological Development**
December, 2020 Vol.4 No.14 7-14

Exergy analysis of the absorption refrigeration cycle using economizers

Análisis exergético del ciclo de refrigeración por absorción utilizando economizadores

VALENCIA-ALEJANDRO, Eric A.[1]†, HERRERA-ROMERO, José V.[1]*, COLORADO-GARRIDO, Darío[2] and SILVA-AGUILAR, Oscar F[1]

[1]Universidad Veracruzana, Facultad de Ingeniería, Avenida Universidad km 7.5, Colonia Santa Isabel, C.P. 96535, Coatzacoalcos, Veracruz 96535, México.
[2]Universidad Veracruzana,Centro de Investigación en Recursos Energéticos y Sustentables, Avenida Universidad km 7.5, Col. Santa Isabel, Coatzacoalcos C.P. 96535, Veracruz, México.

ID 1st Author: *Eric André, Valencia-Alejandro*

ID 1st Coauthor: *José V., Herrera-Romero* / **ORC ID**: 0000-0001-9462-0160, **CVU CONACYT ID**: 163163

ID 2nd Coauthor: *Darío, Colorado-Garrido* / **ORC ID**: 0000-0003-4157-1005, **CVU CONACYT ID**: 171579

ID 3rd Coauthor: *Oscar, Silva-Aguilar* / **ORC ID**: 0000-0002-5109-3193, **CVU CONACYT ID**: 338659

DOI: 10.35429/JTD.2020.14.4.7.14 Received June 26, 2020; Accepted November 28, 2020

Abstract

This paper presents the study of a simple effect absorption refrigeration system (SRA) using the ammonia-water working couple, with the incorporation of three economizers and their analysis of the first and second law of thermodynamics, emphasizing the effect of the operating temperatures and the efficiency of the exchangers on the refrigerant circulation ratio (RC), the coefficient of performance (COP) of the system and the destruction of exergy. In order to determine the thermodynamic properties at each point of the system and evaluate the performance of the SRA, was programmed a tool in MATLAB with the governing equations. The results show that: the exergy efficiency increases when the temperature in the evaporator decreases; and RC decreases with increasing temperature in the generator. As conclusion, an increase in the effectiveness of heat exchangers cannot only decrease the refrigerant circulation rate, but also increase the inlet temperature of the solution to the generator, so that the temperature difference between the solution and the heat source decreases, causing a decrease in the rate of exergy destruction in the generator and the increase in COP.

Second law analysis, Economizers, NH_3-H_2O

Resumen

Este articulo presenta el estudio de un sistema de refrigeración por absorción (SRA) de simple efecto utilizando el par de trabajo amoniaco-agua, con la incorporación de tres economizadores y su análisis de primera y segunda ley de la termodinámica, enfatizando el efecto de las temperaturas de operación y la eficiencia de los intercambiadores en la relación de circulación (RC) de refrigerante, el coeficiente de operación energético (COP) del sistema y la destrucción de exergía. Con el propósito de determinar las propiedades termodinámicas en cada punto del sistema y evaluar el rendimiento del SRA, se programó una herramienta en MATLAB con las ecuaciones gobernantes. Los resultados muestran que: la eficiencia exergética aumenta cuando disminuye la temperatura en el evaporador; y la RC decrece con el aumento de temperatura en el generador. Se concluyó que un aumento de la efectividad de los intercambiadores de calor no solo puede disminuir la tasa de circulación de refrigerante, sino que también aumentar la temperatura de entrada de la solución al generador, por lo que la diferencia de temperatura entre la solución y la fuente de calor disminuye, provocando una disminución de la tasa de destrucción de exergía en el generador y un aumento en el COP.

Análisis de segunda ley, Economizadores, NH_3-H_2O

Citation: VALENCIA-ALEJANDRO, Eric A., HERRERA-ROMERO, José V., COLORADO-GARRIDO, Darío and SILVA-AGUILAR, Oscar F. Exergy analysis of the absorption refrigeration cycle using economizers. Journal of Technological Development. 2020. 4-14: 7-14

* Correspondence to Author (email: vidherrera@uv.mx)
† Researcher contributing first author

Introduction

An absorption refrigeration system (SRA) is a means of cold production that is characterized by operating with a low temperature heat source (Kaynakli and Kilic), so that they can be powered by low-cost alternative energy such as biomass, solar energy, geothermal energy or waste heat. The application of the first law of thermodynamics is very convenient to make a study of the conservation of energy within the system. However, a first law analysis cannot show how or where irreversibilities occur (Aphornratana and Eames). A second law analysis determines the magnitude of irreversible processes in a system, and thus points the direction in which engineers should focus their efforts to improve cycle performance.

The main drawback of an SRA is that energy efficiency is usually very low. The application of technology for the reuse of thermal energy within the system turns out to be a very effective alternative to raise the cycle's operating coefficient.

In this research, the set of equations that model the thermodynamic properties of the system is developed, relying on the MATLAB programming tool for its resolution. In addition to graphically illustrating the results obtained and discussing the importance of using economizers in the cycle to maximize the use of the available energy resource.

System description

Figure 1 shows a schematic diagram of a single-acting SRA. It illustrates the essential components of any absorption refrigeration cycle: absorber, pump, condenser, evaporator, generator, refrigerant expansion valve (VER), and solution expansion valve (VES). SRAs are characterized by the fact that the refrigerant is absorbed by an element on the low pressure side of the system, and released on the high pressure side (Faires and Simmang), referring to the absorber and generator, which replace the compressor of a conventional mechanical refrigeration system. When it comes to the operation of an SRA, a low ammonia, high water content mixture (dilute solution) flows from the generator to the absorber, decreasing its pressure as it passes through the VES in an isentropic manner.

In the absorber, its affinity to ammonia is used to capture refrigerant from the evaporator. The absorption process between the ammonia-water mixture (NH3-H2O) is exothermic, so it is necessary to remove heat to preserve its temperature. To keep the cycle running, the new high-content refrigerant solution (concentrated solution) is pumped to the high-pressure side, where it is heated to the boiling point of the refrigerant, causing ammonia vapor to escape into the condenser, at which is condensed.

Next, the zero quality refrigerant continues its journey through the isentropic VER until it reaches the evaporator with a low temperature. The latent heat necessary for the vaporization of the refrigerant is taken from the space to be cooled, thus creating the desired cooling effect. Finally, the refrigerant vapor flows from the evaporator to the absorber, where it is dissolved in the dilute solution, completing the cycle.

In the studied system, it is proposed to add a solution heat exchanger (ICS) between the concentrated solution that goes to the generator and dilute solution with high temperature that returns from the generator to the absorber. As the temperature of the concentrated solution is increased and the temperature of the dilute solution is reduced, this modification provides a reduction both in the heat supplied in the generator, and in the cooling required by the absorber (Herrera and Colorado).

In the same way, with the intention of reusing the thermal energy that the ammonia vapor has at the generator outlet and that will necessarily have to be dissipated in the condenser, it was proposed to place a solution-refrigerant heat exchanger (ICSR) with what which would increase the temperature of the NH3-H2O mixture coming from the absorber. Similarly, by installing a refrigerant heat exchanger (ICR) in the refrigerant line that leaves the condenser to the evaporator and that goes from the evaporator to the absorber, the cooling effect is increased, subcooling the liquid entering the evaporator.

ISSN 2531-2960

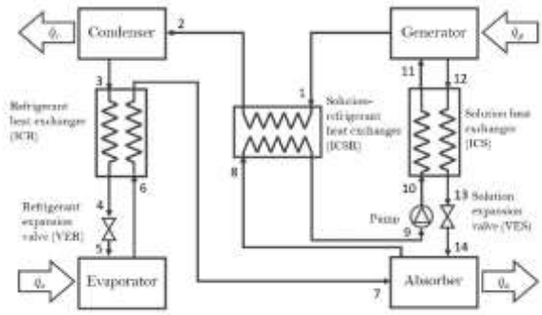

Figure 1 Schematic diagram of the absorption refrigeration cycle with economizers

First law analysis

For each component shown in Figure 1, the balance of energy, mass and matter can be calculated as follows

Generator

$$\dot{Q}_g = \dot{m}_1 h_1 + \dot{m}_{12} h_{12} - \dot{m}_{11} h_{11} \quad (1)$$

$$\dot{m}_1 = \dot{m}_{11} - \dot{m}_{12} \quad (2)$$

$$\dot{m}_1 x_1 = \dot{m}_{11} x_{11} - \dot{m}_{12} x_{12} \quad (3)$$

Condenser

$$\dot{Q}_c = \dot{m}_2 (h_2 - h_3) \quad (4)$$

$$\dot{m}_2 = \dot{m}_3 \quad (5)$$

$$\dot{m}_1 x_1 = \dot{m}_2 x_2 \quad (6)$$

ICR

$$\dot{m}_3 h_3 + \dot{m}_6 h_6 = \dot{m}_4 h_4 + \dot{m}_7 h_7 \quad (7)$$

$$\dot{m}_3 + \dot{m}_6 = \dot{m}_4 + \dot{m}_7 \quad (8)$$

$$\dot{m}_6 x_6 + \dot{m}_3 x_3 = \dot{m}_4 x_4 + \dot{m}_7 x_7 \quad (9)$$

VER

$$\dot{m}_4 h_4 = \dot{m}_5 h_4 \quad (10)$$

$$\dot{m}_4 = \dot{m}_5 \quad (11)$$

$$\dot{m}_4 x_4 = \dot{m}_5 x_5 \quad (12)$$

Evaporator

$$\dot{Q}_e = \dot{m}_6 (h_6 - h_5) \quad (13)$$

$$\dot{m}_5 = \dot{m}_6 \quad (14)$$

$$\dot{m}_5 x_5 = \dot{m}_6 x_6 \quad (15)$$

Absorber

$$\dot{Q}_a = \dot{m}_7 h_7 - \dot{m}_8 h_8 + \dot{m}_{14} h_{14} \quad (16)$$

$$\dot{m}_8 = \dot{m}_7 + \dot{m}_{14} \quad (17)$$

$$\dot{m}_8 x_8 = \dot{m}_{14} x_{14} + \dot{m}_7 x_7 \quad (18)$$

ICSR

$$\dot{m}_1 h_1 + \dot{m}_8 h_8 = \dot{m}_2 h_2 + \dot{m}_9 h_9 \quad (19)$$

$$\dot{m}_1 + \dot{m}_8 = \dot{m}_2 + \dot{m}_9 \quad (20)$$

$$\dot{m}_1 x_1 + \dot{m}_8 x_8 = \dot{m}_2 x_2 + \dot{m}_9 x_9 \quad (21)$$

Pumb

$$\dot{W}_{iso} = \dot{m}_9 (h_{10} - h_9) \quad (22)$$

$$\dot{m}_9 = \dot{m}_{10} \quad (23)$$

$$\dot{m}_9 x_9 = \dot{m}_{10} x_{10} \quad (24)$$

ICS

$$\dot{m}_{10} h_{10} + \dot{m}_{12} h_{12} = \dot{m}_{11} h_{11} + \dot{m}_{13} h_{13} \quad (25)$$

$$\dot{m}_{10} + \dot{m}_{12} = \dot{m}_{11} + \dot{m}_{13} \quad (26)$$

$$\dot{m}_{10} x_{10} + \dot{m}_{12} x_{12} = \dot{m}_{11} x_{11} + \dot{m}_{13} x_{13} \quad (27)$$

VES

$$\dot{m}_{13} h_{13} = \dot{m}_{14} h_{14} \quad (28)$$

$$\dot{m}_{13} = \dot{m}_{14} \quad (29)$$

$$\dot{m}_{13} x_{13} = m_{14} x_{14} \quad (30)$$

The circulation ratio (RC) can be defined as the solution mass flow ratio going from the absorber to the generator ($\dot{m}_{11}$) and the mass flow rate of the refrigerant fluid ($\dot{m}_1$).

$$RC = \frac{\dot{m}_{11}}{\dot{m}_1} = \frac{1 - x_{12}}{x_{11} - x_{12}} \quad (31)$$

Complementary equations

$$\dot{m}_6 = \frac{\dot{Q}_e}{h_6 - h_5} \quad (32)$$

$$\dot{m}_{11} = \left(\frac{1 - x_{12}}{x_{11} - x_{12}} \right) \dot{m}_1 \quad (33)$$

ISSN 2531-2960

$$\dot{m}_{12} = \left(\frac{1 - x_{11}}{x_{11} - x_{12}}\right)\dot{m}_1 \quad (34)$$

For the energy balance in the ICR and ICS, the equations contained in Kilic and Kaynakli were used as a reference, which were adapted to the numbering contained in Figure 1, as shown below

$$h_4 = h_3 - \eta_{ICR}(h_{7-T3} - h_6) \quad (35)$$

$$h_7 = h_6 + \eta_{ICR}(h_{7-T3} - h_6) \quad (36)$$

$$T_{13} = \eta_{ICS} \cdot T_{10} + (1 - \eta_{ICS}) \cdot T_{12} \quad (37)$$

$$h_{10} = h_9 + (P_{11} - P_8)\frac{v_8}{\varepsilon_{bomba}} \quad (38)$$

$$h_{11} = h_{10} + (h_{12} - h_{13})\left(\frac{RC - 1}{RC}\right) \quad (39)$$

The balance for the exchange of energy between the concentrated solution and the refrigerant in the ICSR was carried out according to what was proposed by Karamangil, Coskun, Kaynakli and Yamankaradeniz, as follows

$$h_2 = h_1 - \eta_{ICSR}(h_1 - h_{2-T8}) \quad (40)$$

$$h_9 = h_8 + (h_1 - h_{2-T8})\left(\frac{RC}{\eta_{ICSR}}\right) \quad (41)$$

In the analysis carried out, the concentration and enthalpy properties in the ammonia and water solution were obtained from the relationships provided by Sun. The equation used to determine the entropy of the NH3-H2O mixture was elaborated by Soleymani Alamdari, who used the least squares method to determine the best adjusted equation that would relate the values of previous research and those obtained from simulations carried out by the same. In this way I construct a two-variable equation to calculate the entropy of NH3-H2O under saturated liquid conditions.

The mechanical work done by the pump is defined by

$$W_{me} = \dot{m}_8(P_{11} - P_8)\left(\frac{v_8}{\varepsilon_{bomba}}\right) \quad (42)$$

The performance of the system is measured through the operating coefficient (COP).

$$COP = \frac{\dot{Q}_e}{\dot{Q}_g + \dot{W}_{me}} \quad (43)$$

In general balance, for the first law analysis it must be fulfilled that

$$\dot{Q}_g + \dot{Q}_e + \dot{W}_{me} = \dot{Q}_c + \dot{Q}_a \quad (44)$$

Second law analysis

Exergy is defined as the maximum reversible work that can be obtained from a fluid (Sözen), and it is determined by

$$\dot{E}_i = \dot{m}_i[(h_i - h_0) - T_0(s_i - s_0)] \quad (45)$$

The terms h_0 and s0 represent the enthalpy and entropy values of the fluid involved at ambient temperature T_0.

The variation of exergy within a constant flow system is equal to the exergy transfer minus the exergy destroyed (Panahi and Bozorgan). The exergetic balance for a constant flow system could be expressed as follows

$$\Delta\dot{E} = \sum_{in}\dot{E}_i - \sum_{out}\dot{E}_i + \sum_{in}\dot{Q}\left(1 - \frac{T_0}{T}\right) - \sum_{out}\dot{Q}\left(1 - \frac{T_0}{T}\right) - \dot{W} \quad (46)$$

For each individual component shown in Figure 1, the equation for the rate of variation of exergy is written as follows

$$\Delta\dot{E}_g = \dot{E}_{11} - \dot{E}_1 - \dot{E}_{12} + \dot{Q}_g\left(1 - \frac{T_0}{T_g}\right) \quad (47)$$

$$\Delta\dot{E}_C = \dot{E}_2 - \dot{E}_3 \quad (48)$$

$$\Delta\dot{E}_{ICR} = \dot{E}_3 + \dot{E}_6 - \dot{E}_4 + \dot{E}_7 \quad (49)$$

$$\Delta\dot{E}_{VER} = \dot{E}_4 - \dot{E}_3 \quad (50)$$

$$\Delta\dot{E}_e = \dot{E}_5 - \dot{E}_6 + \dot{Q}_e\left(1 - \frac{T_0}{T_e}\right) \quad (51)$$

$$\Delta\dot{E}_a = \dot{E}_7 + \dot{E}_{14} - \dot{E}_8 \quad (52)$$

$$\Delta\dot{E}_{ICSR} = \dot{E}_8 + \dot{E}_1 - \dot{E}_9 - \dot{E}_2 \quad (53)$$

$$\Delta \dot{E}_{bomba} = \dot{E}_9 - \dot{E}_{10} - \dot{W}_{me} \quad (54)$$

$$\Delta \dot{E}_{ICS} = \dot{E}_{10} + \dot{E}_{12} - \dot{E}_{11} + \dot{E}_{13} \quad (55)$$

$$\Delta \dot{E}_{VES} = \dot{E}_{13} - \dot{E}_{14} \quad (56)$$

The heat discarded to the cooling medium both in the condenser and absorber is neglected because it is energy with a very low exergetic potential due to its proximity to the reference temperature (Gonzales C.). In other words, the energy potential to carry out work that these residues have is minimal and therefore disposable.

The exergetic efficiency of the system is calculated with

$$ECOP = \frac{-\dot{Q}_e\left(1 - \frac{T_0}{T}\right)}{\dot{Q}_g\left(1 - \frac{T_0}{T}\right) + \dot{W}_{me}} \quad (57)$$

Discussion of results

To simplify the analysis of the system, the following considerations were made: (1) due to its low boiling point, it was considered that the concentration and quality of the refrigerant at the generator outlet is pure ammonia in the state of saturated steam; (2) the refrigeration load remains constant at 52.8 kW, which represents approximately 15 tons of refrigeration; (3) the pressure losses, as well as the heat losses / gains along the pipes that connect the equipment are negligible; (4) the system is simulated under steady state conditions; (5) the condenser and absorber temperatures are the same in all cases, that is, $T_a = T_c$.

Table 1 shows the thermodynamic data for the single effect absorption refrigeration system, operating under the following conditions: T_g = 110 ° C; T_e = 5 ° C; $T_c = T_a$ = 40 ° C; T_0 = 25 ° C; $\varepsilon_{pump} = 1$; $\eta_{ICS} = \eta_{ICR} = \eta_{ICSR}$ = 0.8; and 52.8 kW of cooling charge. To solve the equations raised in the previous section, a code was developed in the MATLAB programming environment that uses the database of thermodynamic properties contained in Coolprop. The reference state used for the refrigerant properties was IIR.

Point	T_i (°C)	P_i (kPa)	$x_i\left(\frac{kg\ NH_3}{kg\ sol}\right)$	$\dot{m}_i\left(\frac{kg}{s}\right)$	$h_i\left(\frac{kJ}{s}\right)$	$s_i\left(\frac{kJ}{kg-K}\right)$	E_i (kW)
1	110.000	1554.533	1.000	0.04512	1736.382	5.739	-50.004
2	80.978	1554.533	1.000	0.04512	1614.601	5.530	-52.682
3	40.000	1554.533	1.000	0.04512	390.446	1.644	0.122
4	20.629	1554.533	1.000	0.04512	296.687	1.338	0.000
5	5.000	515.560	1.000	0.04512	296.687	5.555	-56.723
6	5.000	515.560	1.000	0.04512	1466.957	5.555	-3.923
7	41.543	515.560	1.000	0.04512	1560.716	5.139	5.904
8	40.000	515.560	0.503	0.18768	-75.283	1.147	138.659
9	40.001	515.560	0.503	0.18768	-46.008	1.148	144.153
10	46.688	1554.533	0.503	0.18768	-44.954	1.245	138.895
11	84.446	1554.533	0.503	0.18768	138.003	1.770	143.829
12	110.000	1554.533	0.346	0.14257	270.012	1.868	-238.035
13	59.351	1554.533	0.346	0.14257	29.155	1.200	-244.006
14	59.351	515.560	0.346	0.14257	29.155	1.200	-244.006

Table 1 SRA thermodynamic data using working torque NH_3-H_2O

Table 2 shows a comparison between the energy and work loads of the SRA components operating under the same working conditions, but at different levels of efficiency in the exchangers, which operate simultaneously. The sum of heat added to the cycle in the generator and the evaporator, is equal to the sum of heat rejected in the condenser and absorber plus the work done towards the system by the pump.

	$\eta_{IC} = 0.6$	$\eta_{IC} = 0.8$	$\eta_{IC} = 1$
$Q_g\ (kW)$	101.99	90.935	80.827
$Q_c\ (kW)$	57.762	55.231	52.800
$Q_e\ (kW)$	52.800	52.800	52.800
$Q_a\ (kW)$	97.230	88.702	81.021
$W_{me}(kW)$	0.2018	0.1977	0.1939
COP	0.5167	0.5794	0.6517
$ECOP$	0.1663	0.1864	0.2095

Table 2 Results of the first law and second law analysis for an SRA using NH_3-H_2O

For the construction of the graph shown in Figure 2, it was considered that the temperature of the condenser and absorber would remain constant at a value of 40 ° C and multiple temperatures were proposed in the evaporator to compare the thermal load required in the generator. It can be seen how the increase in the generation temperature has a significant impact with a very long slope with the increase in temperature T_g until it reaches an optimal operating temperature and then decreases for a long time. The different values of T_e illustrate that the energy need increases as it is required to reach lower refrigeration temperatures.

From Figure 2, we can conclude that a relatively high temperature heat source produces a lower temperature cooling capacity with a relatively high energy efficiency and a relatively low temperature heat source produces a high temperature cooling capacity with a relatively low energy efficiency.

ISSN 2531-2960

Thus, for example, if the need for cooling was -10 ° C, the best option would be a thermal source of approximately 115 ° C, and if instead of that, a space will need to be conditioned at 5 ° C, the best alternative in this case it would be a thermal source of 90 ° C. Therefore, it is not economical to use a high temperature heat source to obtain high temperature cooling capacity (Cai, He, Tian, & Tang)..

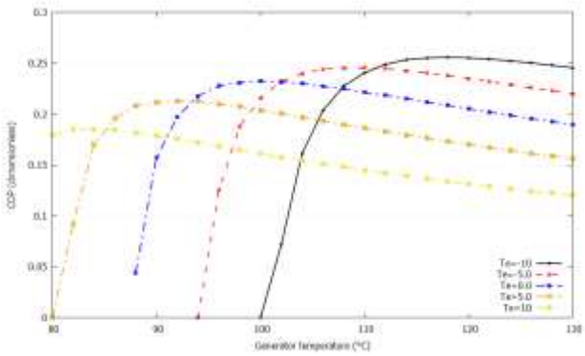

Figure 2 Variation of the coefficient of operation with generator temperature

Figure 3 shows a comparison of the energy efficiency against the generator temperature, in this case at different levels of efficiency in the ICR, ICS and ICSR exchangers, the evaporation temperature considered was 10 ° C. The energy efficiency of the system increases dramatically in the initial stage and then slows down. According to the information presented in Figures 2 and 3, the system increases its performance with the increase in the generation temperature, therefore, the determination of an optimal generation temperature will be a key method to improve the performance of the system. As might be expected, the improvement in the efficiency of the exchangers also has positive consequences in the COP.

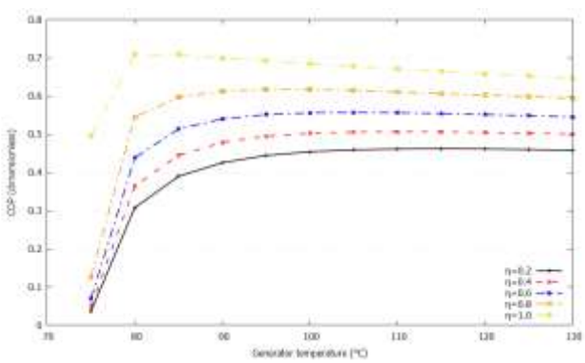

Figure 3 Variation of COP with generation temperature

The effects on the energy operating coefficient that increase the temperature in the absorber, is illustrated in Figure 4, raising the operating temperature of the absorber leads to adverse results in the COP.

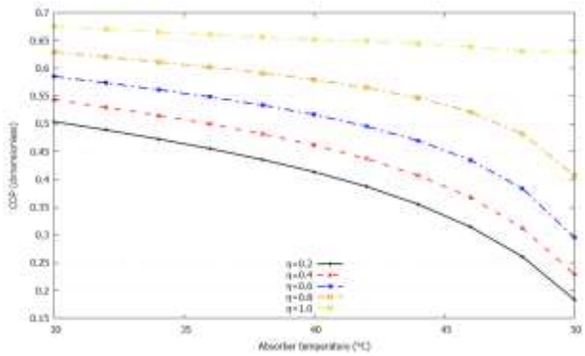

Figure 4 Variation of COP with absorber temperature

The variation of exergy efficiency with generation temperature is shown in Figure 5. Initially, the efficiency increases dramatically and then decreases as T_g increases. Taking into account that the temperature in the evaporator remains constant in this graph, it follows that there is no single optimal generation temperature for maximum exergetic use, but rather that it varies around the efficiency of the economizers. On the other hand, the graph indicates that the lowest irreversibilities are achieved with the highest efficiency levels of the exchangers.

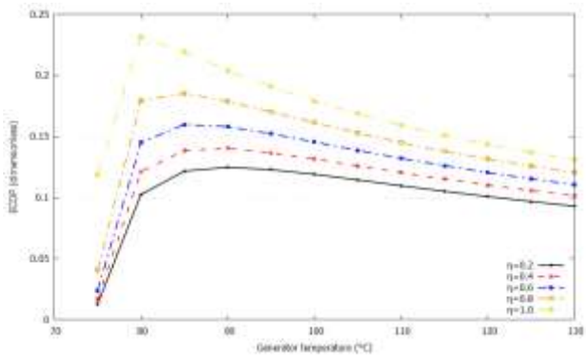

Figure 5 Variation of the exergetic operating coefficient with the generator temperature

The graph shown in Figure 6 was developed at different generation temperatures to analyze the behavior of the ECOP against the evaporator temperature. In view of the fact that, under the same temperature conditions of the generator and condenser, the exergetic efficiency increases with the increase in the evaporator temperature and then decreases, it is concluded that, for each ECOP curve against T_e there is a maximum value of exergetic efficiency

.

That is, when T_g, T_c and T_a are specified, there must be an optimal value of evaporator temperature T_e, below which the maximum energy of the system is used. In practice, the evaporator temperature is usually a known data that is determined by the requirements of the process, and the generation temperature is usually not difficult to adjust to achieve an optimal operating state of the system..

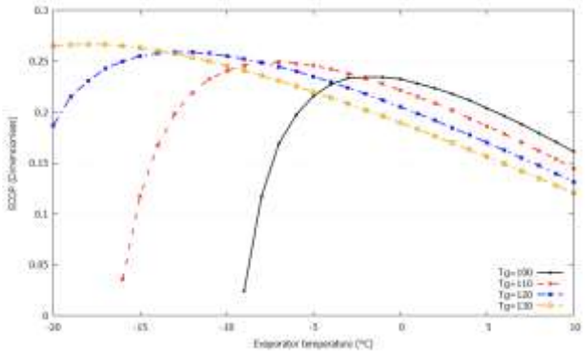

Figure 6 Variation of the exergy operating coefficient with evaporator temperature

As can be seen in Figure 7, the exergy destroyed in both the evaporator and the condenser tiny in relation to the exergy produced in the generator or that destroyed in the absorber. The exergy trend in the generator indicates that the energy needed to complete the refrigeration cycle decreases as the efficiency in the exchangers improves, likewise, the exergy destroyed in the absorber decreases.

What has been said so far supposes that the energy reused at the generator output, both in the ICSR and in the ICS, increases the temperature of the mixture at its inlet, reducing the thermal load required for the boiling of the refrigerant. Likewise, the energy transferred in the ICR and ICS, reduce the amount of heat to disperse in the absorber.

The latter represents an advantage, because it increases the absorption capacity, since by itself, the mixture between refringent and absorbent represents an exothermic process that reduces its dissolution capacity as its temperature increases. As both the diluted solution and the refrigerant enter the absorber at lower temperatures than they would have without the existence of the exchangers, the resulting mixture has a higher concentration of ammonia.

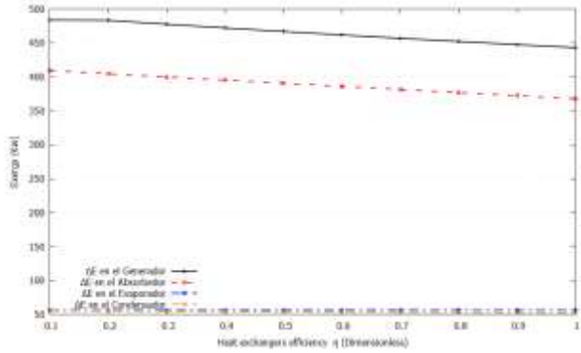

Figure 7 Exergy in the generator, absorber, evaporator and condenser, against the heat exchangers efficiency

Conclusion

In this work, the first and second laws of thermodynamics were applied to a SRA with economizers. The operation of the cycle and the effects of the addition of exchangers were described, as well as the equations that model the cycle from an energetic and exergetic aspect. In addition, a numerical example was made in which the thermodynamic properties of each state indicated in Figure 1 were defined.

It is concluded then that the decrease in the thermal load on the generator increases the COP. As demonstrated in this research, better thermodynamic performances can be achieved by supplying low-grade residual heat than by operating with excess temperatures in the generator. From the exergy study, it can be inferred that the best way to increase cycle efficiency is by optimizing the economizers. It is clear that, by increasing the energy transfer rate that is recovered at the generator output, the energy destroyed in both the absorber and the condenser is reduced, causing an improvement in the ECOP. In addition to this, the recirculation of heat towards the generator reduces the energy load required for generation, making the cycle more economically attractive.

The main priority to improve the efficiency of the cycle should be to improve the efficiency of the exchangers and secondly, to modify the evaporator temperature. However, as the T_e value is usually a set value, subject to the needs of a process, it is recommended to delegate that responsibility to the generator.

ISSN 2531-2960

Nomenclature

$\dot{m}$	Mass flow [kg / s]
x	Concentration [Kg of refrigerant / kg of solution]
P	Pressure [Pa]
T	Temperature [° C]
h	Enthalpy [J / kg]
s	Entropy [J / Kg-K]
v	Specific volume [m ^ 3 / kg]
$\dot{E}$	Exergy flow [kW]
$\dot{Q}$	Heat flow [kW]
$\dot{W}$	Work [kW]
η	Efficiency
ε	Effectiveness

Subscripts

g	Generator
a	Absorber
e	Evaporator
c	Condenser
ICS	Solution heat exchanger
ICR	Refrigerant heat exchanger
$ICSR$	Solution-refrigerant heat exchanger
iso	Isoentropic
me	Mechanical
i	Status points
0	Dead state

References

Kaynakli, O., & Kilic, M. (2007). Theoretical study on the effect of operating conditions on performance of absorption refrigeration system. Energy Conversion and Management, 48(2), 599-607.

Aphornratana, S., & Eames, I. W. (1995). Thermodynamic analysis of absorption refrigeration cycles using the second law of thermodynamics method. International journal of refrigeration, 18(4), 244-252.

Faires, V. M., & Simmang, C. M. (1983). Termodinámica. 6. México: Uteha.

Herrera-Romero, J. V., & Colorado-Garrido, D. (2020). Comparative Study of a Compression–Absorption Cascade System Operating with NH3-LiNO3, NH3-NaSCN, NH3-H2O, and R134a as Working Fluids. Processes, 8(7), 816:831.

Kilic, M., & Kaynakli, O. (2007). Second law-based thermodynamic analysis of water-lithium bromide absorption refrigeration system. Energy, 32(8), 1505-1512.

Karamangil, M. I., Coskun, S., Kaynakli, O., & Yamankaradeniz, N. (2010). A simulation study of performance evaluation of single-stage absorption refrigeration system using conventional working fluids and alternatives. Renewable and Sustainable Energy Reviews, 14(7), 1969-1978.

Sun, D. W. (1998). Comparison of the performances of NH3-H2O, NH3-LiNO3 and NH3-NaSCN absorption refrigeration systems. Energy Conversion and Management, 39(5-6), 357-368.

Soleymani, A. G. (2007). Simple equations for predicting entropy of ammonia-water mixture.

Sözen, A. (2001). Effect of heat exchangers on performance of absorption refrigeration systems. Energy Conversion and Management, 42(14), 1699-1716.

Panahi, Z. F., & Bozorgan, N. (2011). The energy and exergy analysis of single effect absorption chiller.INT J Advanced Desing and manufacture Technology, 4(4), 19-26.

Gonzáles C., Israel (2014). Análisis exergético del sistema de refrigeración por absorción regenerativo NH3-H2O (Tesis de pregrado). Universidad Nacional Autónoma de México, Distrito Federal, México.

Cai, D., He, G., Tian, Q., & Tang, W. (2014). Exergy analysis of a novel air-cooled non-adiabatic absorption refrigeration cycle with NH3–NaSCN and NH3–LiNO3 refrigerant solutions. Energy conversion and management, 88, 66-78.

ISSN 2531-2960

Artícle **Journal of Technological Development**
December, 2020 Vol.4 No.14 15-19

Mathematical modeling of the diffusion of liquids in the gaseous phase by evaporation

Modelado matemático de la difusión de líquidos en fase gaseosa por evaporación

LOPEZ-VALDIVIESO, Leticia†*, ELISEO-DANTÉS, Hortensia, CASTRO-DE LA CRUZ, Jucelly and TEJERO-RIVAS, María Candelaria

Tecnológico Nacional de México/Instituto Tecnológico de Villahermosa

ID 1st Author: *Leticia, López-Valdivieso* / **ORC ID**: 0000-0001-6288-3636, **Researcher ID Thomson**: G-5753-2018, **CVU CONACYT ID**: 67839

ID 1st Coauthor: *Hortensia, Eliseo-Dantés* / **ORC ID**: 0000-0003-4006-4669, **Researcher ID Thomson**: F-6749-2018, **CVU CONACYT ID**: 411079

ID 2nd Coauthor: *María Candelaria, Tejero-Rivas* / **ORC ID**: 0000-0002-1753-0767, **Researcher ID Thomson**: ABC-2057-2020, **CVU CONACYT ID**: 668744

ID 3rd Coauthor: *Jucelly, Castro-De La Cruz* / **ORC ID**: 0000-0002-3862-9555, **Researcher ID Thomson**: G-1886-2018, **CVU CONACYT ID**: 739319

DOI: 10.35429/JTD.2020.14.4.15-19 Received June 26, 2020; Accepted November 28, 2020

Abstract

The objective of this study is to analyze the behavior of liquid molecules during an evaporation process, a mathematical model is proposed through mass a balance that describes said behavior under steady-state conditions and the variation in composition is analyzed in detail, through a finite space. In order to know the concentration profile, it is necessary to characterize the behavior of the moisture present in the medium as part of the parameters that affect the system, which will at the same time allow knowing the molar composition of the water present in the medium or system of study. Temperature is another of the variables of great importance in the evaporation process, which is why a variation of the concentration profile will occur at different temperatures.

Evaporation, Profile, Concentration

Resumen

El objetivo de este estudio es analizar el comportamiento de las moléculas del líquido durante un proceso de evaporación, se plantea a través de balances de materia un modelo matemático que describe dicho comportamiento bajo condiciones de estado estable y se analiza a detalle la variación de la composición a través de un espacio finito determinado. Con el fin de conocer el perfil de concentración es necesario caracterizar el comportamiento de la humedad presente en el medio como parte de los parámetros que afectan el sistema, lo que permitirá a la vez saber la composición molar del agua presente en el medio o sistema de estudio. La temperatura es otra de las variables de gran importancia en el proceso de evaporación por lo que se presentará una variación del perfil de concentración a diferentes temperaturas.

Evaporación, Perfil, Concentración.

Citation: LOPEZ-VALDIVIESO, Leticia, ELISEO-DANTÉS, Hortensia, CASTRO-DE LA CRUZ, Jucelly and TEJERO-RIVAS, María Candelaria. Mathematical modeling of the diffusion of liquids in the gaseous phase by evaporation. Journal of Technological Development. 2020. 4-14: 15-19

* Correspondence to Author (email: leticia.lv@villahermosa.tecnm.mx)
† Researcher contributing first author

Introduction

Evaporation is an essential part of the water cycle, solar energy accelerates the evaporation process. For the molecules of a liquid to evaporate, they must be located near the surface, move in the proper direction, and have enough energy to overcome the intermolecular forces of the liquid phase. Not all molecules meet these criteria, this is the cause of the limited evaporation of these molecules. The kinetic energy of a molecule is proportional to its temperature, evaporation takes place more rapidly as the temperature is higher, because the faster-moving molecules escape, the remaining molecules have a lower average kinetic energy, and therefore the temperature of the liquid decreases. Three key factors affect evaporation: heat, humidity, and air movement.

A more detailed analysis of the factors that influence the evaporation rate allows us to recognize that: a) if the air has a high concentration of the evaporating substance, then the substance will evaporate more slowly, b) if the liquid contains other substances , it will have a lower capacity for evaporation, c) The temperature allows to accelerate the evaporation process, so if the temperature rises the evaporation will be faster, d) the greater the forces that hold the molecules together in the liquid, more energy will be needed to evaporate them, and e) a substance that has a larger surface area will evaporate faster, since there are more surface molecules that are able to escape.

In general, considering the evaporation of a free water surface (lake, river, lagoon, etc.) as the simplest form of the process, this is carried out as follows: The water molecules are in continuous movement, When they reach the surface of the liquid, they are heated by the effect of solar radiation, they increase their temperature and consequently their speed, thus increasing their kinetic energy, until some manage to free themselves from the attraction of adjacent molecules and cross the interface. liquid-gas, turning into vapor. However, the layer of air immediately on the surface becomes saturated soon and the reverse process occurs simultaneously with evaporation, so the molecules condense and return to the liquid state.

The difference between the number of molecules that leave the liquid and the number of molecules that return to it, marks the global nature of the phenomenon. If it is positive, evaporation occurs. If negative, condensation.

Methodology

According to the Conagua records through the National Meteorological Service prevailing in the state of Tabasco, it is possible to obtain information that allows establishing the mechanisms for analyzing the current situation regarding the behavior of temperature and relative humidity. The percentage of relative humidity will allow knowing the partial pressure of the air, in order to subsequently evaluate the molar composition of the air at the conditions prevailing in the state.

It is also necessary to know the molar composition of the liquid on the surface, that is to say at the liquid-gas interface, for this the vapor pressure of the water at the temperature at which said mass of liquid must be found is evaluated. With this information and knowing the total pressure that governs the state, which is at sea level, the molar composition at the interface is evaluated.

The proposed mathematical model that defines the behavior of the composition through a defined height, arises from applying a microscopic mass balance in a small differential element located in the liquid transfer zone, that is, in the region it occupies specifically air. This balance is carried out according to the principles of mass transfer, where it is known that there is no accumulation of matter in the system. It is necessary to know two specific conditions in said system, which will allow evaluating the integration constants that arise from the applied balance.

Finally, the mathematical equation obtained will allow to model the variation in the composition of the liquid from the area of the liquid-gas interface, up to a defined height that will be found precisely within the air.

When graphing the equation, it will be observed how said variation is affected by temperature, air speed, air humidity and the extended surface of said mass of liquid.

ISSN 2531-2960

LOPEZ-VALDIVIESO, Leticia, ELISEO-DANTÉS, Hortensia, CASTRO-DE LA CRUZ, Jucelly and TEJERO-RIVAS, María Candelaria. Mathematical modeling of the diffusion of liquids in the gaseous phase by evaporation. Journal of Technological Development. 2020

Analysis of previous data

The results obtained from the relative humidity in the state of Tabasco during 25 days of the month of April of the year 2019, are concentrated in the following table:

Day	Temperature [ºC]	Relative Humidity (RH) [%]
01	21.9	86.9
02	22.9	89.3
03	25.8	76.5
04	26.4	78.2
05	28.8	62.4
06	28.9	64.1
07	28.8	66.6
08	29.0	67.7
09	25.9	77.8
10	26.1	68.0
11	27.7	59.0
12	29.1	61.5
13	31.1	50.3
14	24.7	59.9
15	25.4	69.7
16	28.0	70.3
17	28.2	73.7
18	30.0	61.6
19	26.7	66.5
20	25.1	61.0
21	26.3	53.5
22	29.9	59.8
23	28.0	67.2
24	29.3	60.9
25	29.9	60.5

Table 1 Temperature and Relative Humidity of the municipality of Centro in the state of Tabasco from April 01 to 25, 2019
Source: History of the climate in Villahermosa (https://www.meteored.mx/villahermosa/historico)

The secondary information source that was used allowed to evaluate the daily averages of temperature and relative humidity that were stored and processed in a database, to later be useful for the calculation and processing bases of all the information generated until the elaboration of the graphs of the final results.

Results

The data collected and concentrated in Table 1, allowed to evaluate the partial pressure of the water vapor in the prevailing region on the surface of the water, considering for these calculations only two temperature values (20oC and 25oC), both the partial pressure values Since the molar fraction (yA) present very little variation, therefore, for the purposes of this calculation procedure.

An average of the total of the 25 values that were evaluated will be taken, it should be noted that the molar fraction reported in said Table was evaluated considering a total pressure of 101,325 kPa.

T = 20°C Partial Pressure, P_A [kPa]	y_{A2}	T = 25°C Partial Pressure, P_A [kPa]	y_{A2}
2.0433	0.0202	2.7701	0.0273
2.0997	0.0207	2.8466	0.0281
1.7987	0.0178	2.4386	0.0241
1.8387	0.0181	2.4928	0.0246
1.4672	0.0145	1.9891	0.0196
1.5072	0.0149	2.0433	0.0202
1.5660	0.0155	2.1230	0.0210
1.5918	0.0157	2.1581	0.0213
1.8293	0.0181	2.4800	0.0245
1.5989	0.0158	2.1676	0.0214
1.3873	0.0137	1.8807	0.0186
1.4460	0.0143	1.9604	0.0193
1.1827	0.0117	1.6034	0.0158
1.4084	0.0139	1.9094	0.0188
1.6389	0.0162	2.2218	0.0219
1.6530	0.0163	2.2410	0.0221
1.7329	0.0171	2.3493	0.0232
1.4484	0.0143	1.9636	0.0194
1.5636	0.0154	2.1198	0.0209
1.4343	0.0142	1.9445	0.0192
1.2579	0.0124	1.7054	0.0168
1.4061	0.0139	1.9062	0.0188
1.5801	0.0156	2.1421	0.0211
1.4319	0.0141	1.9413	0.0192
1.4225	0.0140	1.9286	0.0190

Table 2 Partial pressures evaluated from the temperature and relative humidity data in the municipality of Centro in the state of Tabasco from April 01 to 25, 2019
Source: Author's contribution (April 2019)

Calculating the average of the reported values we have:

T = 20°C		T = 25°C	
Average Partial Pressure, P_A [kPa]	$y_{A2(average)}$	Average Partial Pressure, P_A [kPa]	$y_{A2(average)}$
1.5734	0.0155	2.1331	0.0211

Table 3 Partial pressure and average molar fraction for the calculation of the concentration profile
Source: Author's contribution (April 2019)

Vapor pressure is evaluated at the temperature at which the evaporating liquid is, in this case, for this study the average temperatures reported for rivers in the state are taken. Fluctuating the values between a range of 20 to 35 ° C, for which four different temperatures were analyzed, presented below:

ISSN 2531-2960

Temperature [ºC]	Vapor pressure (P_{AV}) [kPa]	y_{A1}
20	2.3513	0.0232
25	3.1877	0.0315
30	4.2715	0.0422
35	5.6609	0.0559

Table 4 Vapor pressures evaluated at four different temperatures and corresponding mole fraction
Source: Author's contribution (April 2019)

The matter balance applied to a differential element of finite thickness in the air zone is established without accumulation of matter, and the equations that govern this behavior are presented below:

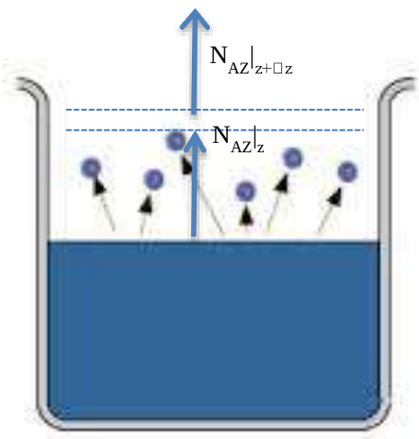

General balance of matter:

$$E - S = 0 \quad (1)$$

$$N_A|z - N_A|_{z+\Delta z} = 0 \quad (2)$$

This balance generates the following differential equation, (dividing equation 2 by ΔZ and applying limits):

$$\frac{dN_A}{dz} = 0 \quad (3)$$

By introducing the corresponding general equation of molecular diffusion flow for the case that corresponds to this diffusion phenomenon, which is: Diffusion of "A" through "B" at rest, we have:

$$N_A = -\frac{cD_{AB}}{(1-y_A)}\frac{dy_A}{dz} \quad (4)$$

$$\frac{d}{dz}\left(-\frac{cD_{AB}}{(1-y_A)}\frac{dy_A}{dz}\right) = 0 \quad (5)$$

This differential equation is solved by separation of variables, considering that both the total concentration and the diffusivity of the system (c and D_{AB}) are constant and it is possible to treat them mathematically to integrate this equation twice; and obtain the following equation as a result:

$$-Ln\,(1-y_A) = c_1 z + c_2 \quad (6)$$

The constants of integration are evaluated by applying the prevailing system conditions in the environment, which are:

Para $z = 0$ $y_A = y_{A1}$

Para $z = 0.5$ m $y_A = y_{A2}$

According to these it is possible to know the value of the constants and obtain the concentration profiles.

It is important to point out that once the integration constants are known, it is possible to obtain a general equation that outlines the behavior of the concentration of "A", through the height z, and the concentration of B is obtained by difference, as shown in graph 1.

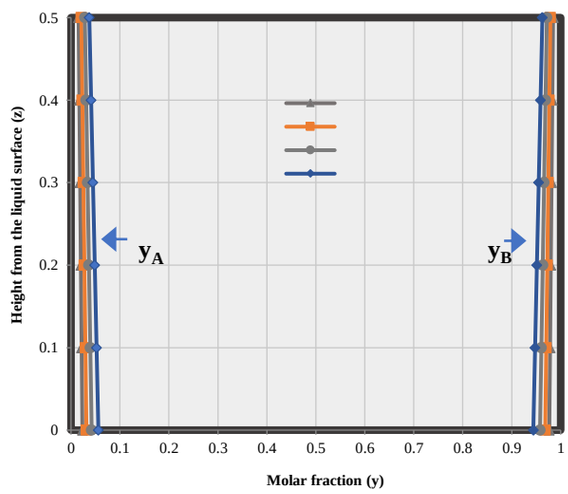

Graphic 1 Composition profile of water through air at different temperatures
Source: Author's contribution (April 2019)

The plotted concentration profiles were evaluated for four different temperatures of the evaporating liquid, the calculations are based on the relative humidity, the partial pressure and the integration constants of equation (6).

ISSN 2531-2960

Conclusions

The study of the behavior of the molecules during a vaporization process through a gas phase is of utmost importance in order to know the variation of the composition in transfer zones that allow an acceleration of the diffusion process. The amount of molecules that evaporate to a liquid phase is significantly dependent on relative humidity and temperature. The results of this study show that there is little variation in the composition of water through the air, observing an area of higher concentration just on the surface of the liquid. The model obtained from the balance presents a good prediction of the concentration profile. It should be noted that even when the relative humidity was 100%, this profile does not present much variation, results that were obtained with great reliability in the application of the model.

References

Bird, R.B., Stewart, W.E., Lightfoot, E.N.,(1992). Fenómenos de Transporte. Ed. Reverté.

Hines, L., A., Maddox, N., R., (1987), Transferencia de Masa, Fundamentos y Aplicaciones. Prentice-Hall Hispanoamericana, S.A.

Manzur, A. y Cardoso J. (2015). Velocidad de Evaporación del agua. Revista Mexicana de Física. *61*, 31-34.

Meteored. *Histórico del clima en Villahermosa*. https://www.meteored.mx/villahermosa/historico

Reporte del Clima en México. (2019). Coordinación General del Servicio Meteorológico Nacional. CONAGUA.

ISSN 2531-2960

Artícle **Journal of Technological Development**
December, 2020 Vol.4 No.14 20-27

Turbidity, dissolved Oxygen and pH measurement system for grey water treatment process by electrocoagulation

Sistema de medición de turbidez, oxígeno disuelto y pH para el proceso de tratamiento de aguas grises por electrocoagulación

CANTERA-CANTERA, Luis Alberto†*, CALVILLO-TÉLLEZ, Andrés and LOZANO-HERNANDEZ, Yair

Instituto Politécnico Nacional, Escuela Superior de Ingeniería Mecánica y Eléctrica.

ID 1st Autor: *Luis Alberto, Cantera-Cantera* / **ORC ID**: 0000-0003-2828-6779

ID 1st Coautor: *Andrés, Calvillo-Téllez* / **ORC ID**: 0000-0003-3721-5630

ID 2nd Coautor: *Yair, Lozano-Hernández* / **ORC ID**: 0000-0001-8157-3510

DOI: 10.35429/JTD.2020.14.4.20.27 Received June 26, 2020; Accepted November 28, 2020

Abstract

Electrocoagulation is an electrochemical process used to treat wastewater and water contaminated with heavy metals. This method destabilizes contaminants that are suspended, emulsified or dissolved in wastewater by applying electrical current through electrodes and then removing them by filtration. In this work we present a turbidity, dissolved oxygen and pH measurement system for the influent and effluent of the gray water treatment process by the electrocoagulation method. The treatment process is carried out via batch and the measurement system allows to know the initial and final levels of the variables through a human machine interface (HMI) designed in LabVIEW. Twelve experimental tests were performed varying the treatment time and applied voltage in the electrocoagulation process to analyze the rate of change of the measured variables and its behavior regarding time and voltage. The applied direct current voltages were 10 V, 15 V and 20 V during 30 min, 60 min, 90 min and 120 min.

Electrocoagulation, Grey Water Treatment, Measurement System

Resumen

La electrocoagulación es un proceso electroquímico utilizado para tratar aguas residuales y agua contaminada con metales pesados. Este método desestabiliza los contaminantes que están suspendidos, emulsionados o disueltos en las aguas residuales aplicando corriente eléctrica a través de electrodos y luego eliminándolos por filtración. En este trabajo se presenta un sistema de medición de turbidez, oxígeno disuelto y pH para el afluente y efluente del proceso de tratamiento de aguas grises por el método de electrocoagulación. El proceso de tratamiento se realiza vía batch y el sistema de medición permite conocer los niveles inicial y final de las variables a través de una interfaz hombre-máquina (HMI) diseñada en LabVIEW. Se realizaron doce pruebas experimentales variando el tiempo de tratamiento y la tensión aplicada en el proceso de electrocoagulación para analizar la tasa de cambio de las variables medidas y su comportamiento en cuanto a tiempo y tensión. Los voltajes de corriente continua aplicados fueron 10 V, 15 V y 20 V durante 30 min, 60 min, 90 min y 120 min.

Electrocoagulación, Tratamiento de aguas grises, Sistema de medición

Citation: CANTERA-CANTERA, Luis Alberto, CALVILLO-TÉLLEZ, Andrés and LOZANO-HERNANDEZ, Yair. Turbidity, dissolved Oxygen and pH measurement system for grey water treatment process by electrocoagulation. Journal of Technological Development. 2020. 4-14: 20-27

* Correspondence to Author (email: lcanterac@ipn.mx)
† Researcher contributing first author

Introduction

According to United Nations (UN) information [1], due to the water scarcity and poor water quality by 2050 at least one in four people is likely to live in a country affected by chronic or recurring shortages of freshwater. A sustainable development goal for UN is clean water and sanitation to ensure availability and sustainable management of water and sanitation for all and also halving the proportion of untreated wastewater and substantially increasing recycling and safe reuse globally [1]. In this sense, the electrocoagulation (EC) for wastewater treatment is a choice. Different studies and applications have demonstrated its effectiveness [2, 3, 4, 5, 6, 7, 16]. On the other hand, a very important part for any wastewater treatment process is the knowledge of the degree of pollution that water presents.

The degree of water pollution is determined by the permissible levels of its physical, chemical and biological characteristics established in national and international standards, for example [8, 9]. Some of this characteristics are turbidity, temperature, conductivity, pH, alkalinity and colloids, dissolved oxygen (DO), biochemical and chemical oxygen demand, and its knowledge will allow to establish a quality control of the treated water and to detect alterations in the treatment process. Most of the studies that use EC for water treatment show the analysis of the following variables: current and voltage applied, size and material used on the electrodes, distance between electrodes, pH, temperature and conductivity of water and operating costs [4, 16].

However, the physical, chemical and biological characteristics of water have not been studied enough [4]. Hence we design a turbidity, dissolved oxygen and pH measurement system for the influent and effluent. For the gray water treatment process using the EC method to analyze its behavior for different treatment times and applied voltages through a human machine interface (HMI) designed in LabVIEW. As far as the authors know, this is the first time that a measurement system of analytic variables is applied to the gray water treatment by electrocoagulation.

The structure of this work is as follows: Section 2 describes the basic equipment to carry out the EC and the treatment process designed. Section 3 describes the measurement system equipment used, the HMI and its sequential operation. Finally, section 4 shows the turbidity, dissolved oxygen and pH measurement data from twelve experimental test and then concluding remarks.

Methodology of Wastewater Treatment Process by EC

Several studies such as [2, 6, 7] define the different reactions and mechanisms involved during the EC but the main reaction involves a continuously dissolving anode due to the passage of electricity, releasing cations into the wastewater. On the other hand, considering several applications such as [10, 11, 12, 13, 14] the basic equipment to carry out the EC are 1) electrochemical reactor, 2) sacrificial electrodes and 3) direct current electrical power supply as shown in Figure 1.

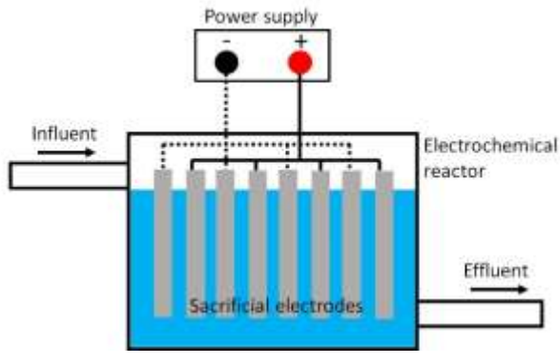

Figure 1 Basic equipment for EC.
Source: Own Elaboration

The proposed gray water treatment process using EC is carried out via batch and we design the treatment process shown in Figure 2 which adds two storage tanks where the turbidity, dissolved oxygen and pH measurements will be made.

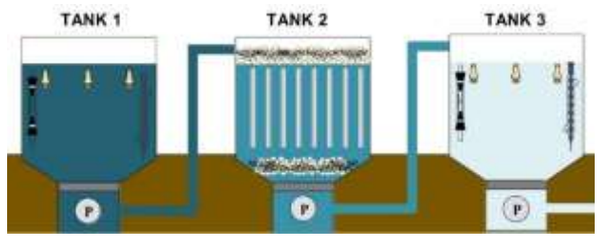

Figure 2 Treatment process
Source: Own Elaboration

The process has three stages, each of them carried out in each tank of the Figure 2 and sequentially. In the first stage (tank 1) the pH, dissolved oxygen and turbidity measurement is carried out on the gray water, later the EC is carried out in the second stage (tank 2) finally in the third stage (tank 3) the pH, dissolved oxygen and turbidity measurement is carried out on the treated water. The electrochemical reactor used in this process has a maximum treatment capacity of 9 L, its components are shown in Figure 3.

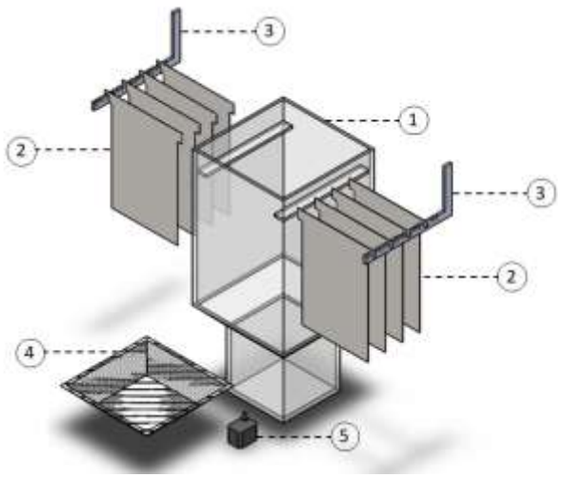

Figure 3 Electrocoagulation equipment. 1) Electrochemical reactor, 2) Sacrificial electrodes, 3) Power terminals, 4) Strainer filter, 5) Pump.
Source: Own Elaboration

Development

The measurement stages are carried out in tanks 1 and 3, each of them with the components shown in Figure 4. Each measurement stage has 3 turbidity sensors, 1 dissolved oxygen sensor and 1 pH sensor, a brief description the sensors used is shown below.

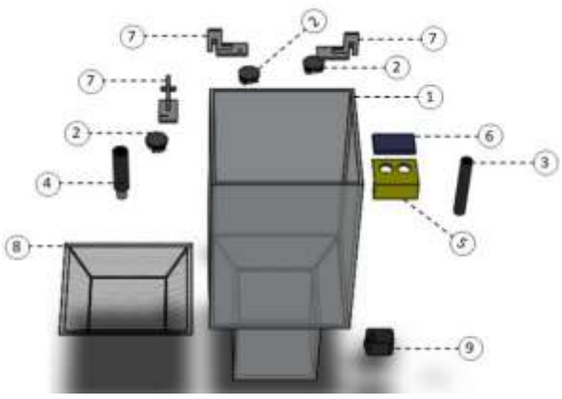

Figure 4 Measurement stage. 1) Tank, 2) Turbidity sensor, 3) Dissolved oxygen sensor, 4) pH sensor, 5) Level sensor support, 6) Level sensor, 7) Turbidity sensor support, 8) Strainer filter, 9) Pump
Source: Own elaboration

3.1 Turbidity Sensor

Some particles such as clays, inorganic matter, salts, soluble color compounds and microorganisms affect water clarity. Turbidity is a transparency degree measurement in a liquid and it is an indicator of water pollution [8, 9]. It is measured in Nephelometric Turbidity Units (NTU) by a nephelometer or turbidimeter, which measures the intensity of light scattered as a beam of light passes through a water sample. The turbidity sensor used in this work is Gravity arduino turbidity sensor and its documentation can be found in [17].

3.2 Dissolved Oxygen Sensor

DO is an indicator of pollution [8, 9], generally a higher level of dissolved oxygen that indicates better water quality [5] to support plant and animal life. The OD sensor is a galvanic probe, which measure the oxygen content of water in mg/L using an electrochemical method [21]. In this work the sensor used is Gravity analog that dissolved oxygen sensor and its documentation can be found in [18].

3.3 pH Sensor

The pH is an index of the hydrogen ion concentration H+ in water and it is an important variable in water quality [22]. It is a measure of acidity and alkalinity of a solution, which is based on logarithmic transformation of the hydrogen ion concentration. It has a scale ranging from 0-14, where the value 7 represents neutrality. Solutions with a pH above 7 are alkaline, while below 7 are acidic. The pH sensor used is Gravity analog and documentation for pH sensor can be found in [19].

The principal technical characteristics of the sensors are shown in Table. On the other hand, the signal acquisition of all sensors is carried out by a microcontroller ATMEGA 2560 its documentation can be found in [20].

3.4 Human Machine Interface

The sensors signals processing and operation of the process is carried out by a human machine interface (HMI) designed in LabVIEW [23]. Due to LabVIEW graphical programming language, it is easy to create flexible interfaces to changes and needs. The HMI is divided in three sections: tanks, measurement and control.

ISSN 2531-2960

Variable	Sensor	Technical characteristics
DO	Gravity analog dissolved oxygen sensor DFRobot	Measuring Range: 0-20 mg/L Analog Signal Output: 0-3 V Membrane Cap Replacement Period: 1-2 months in muddy water
pH	Gravity pH sensor DFRobot	Measuring Range: 0-14pH Measuring Precision: ≤0.02pH Drift: ≤0.02pH/24hours
Turbidity	Gravity arduino turbidity sensor DFRobot	Measuring Range: 0-3000 NTU Analog output: 0-4.5 V Turbidity-Voltage relationship: -1120.4V2+5742.3V-4352.9

Table 1 Sensors technical characteristics
Source: Own Elaboration

In Figure 5, red line indicates the tanks section, when the treatment process is running, the HMI has visual indicators of the current status of tank levels and pump activation. Blue and green lines indicate the measurement section for the measurement stages 1 and 2 respectively, at each measurement stages, turbidity is measured first, then pH and finally dissolved oxygen. The yellow line indicates the control section, it has a start selector for automatic mode, an emergency stop button, a button to select manual mode and another to exit, it also has a selector to take measurements when the process is in manual mode.

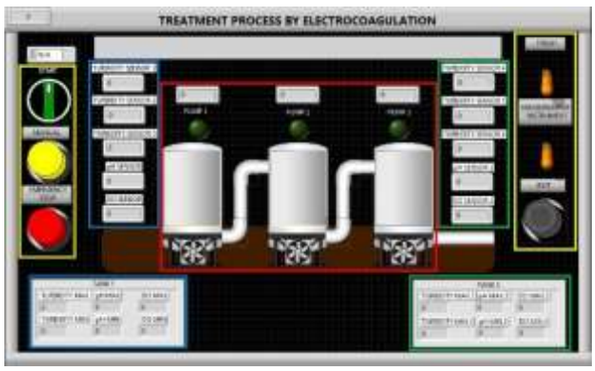

Figure 5 Treatment process interface
Source: Own Elaboration

4 Experiments and Results

Experimental tests were performed under the following considerations: The electrodes used were aluminum with dimensions of 220 mm length, 170 mm width and 1 mm thickness, eight electrodes were used in parallel monopolar connection (see Figure 1) and they were separated by a space of 10 mm. More details about electrode connections consult [2].

The wastewater used was grey water from a laundry. The applied voltages were 10 V, 15 V and 20 V during 30 min, 60 min, 90 min, and 120 min. During the experiment tests the electrodes and the strainer filter in the electrochemical reactor were cleaned after each experiment. Also, before carried out experiments 5, 8 y 12 the electrochemical reactor was cleaned and before experiment 8, four central electrodes were replaced. The sensors and the treatment process setup are shown in Figures 6 and 7 respectively.

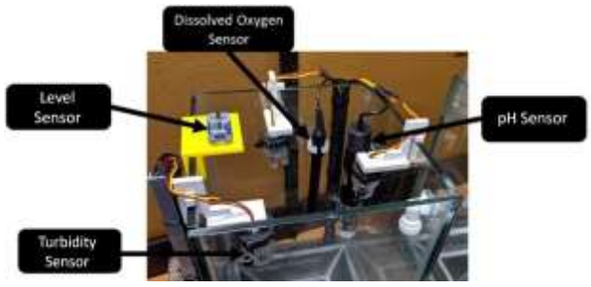

Figure 6 Sensors setup.
Source: Own Elaboration

Figure 7 Treatment process setup.
Source: Own Elaboration

Table 2 shown the DO and pH experimental measurements, in Tables 3 and 4 are shown the influent and effluent turbidity experimental measurement in NTU, respectively.

	Time [min]	Voltage [V]	Influent [mg/L]	Effluent [mg/L]	Influent [pH	Effluent [pH]
1	30	10 V	0.135	0.480	7.709	7.635
2	60	10 V	0.128	0.487	7.757	8.852
3	90	10 V	0.122	0.507	7.823	9.288
4	120	10 V	0.115	0.520	7.786	8.730
5	30	15 V	0.460	0.890	7.280	7.650
6	60	15 V	0.450	1.080	8.010	8.100
7	90	15 V	0.330	0.820	7.980	9.130
8	120	15 V	0.350	0.910	7.970	9.150
9	30	20 V	0.480	0.950	7.900	7.990
10	60	20 V	0.550	1.100	8.010	8.840
11	90	20 V	0.600	1.150	8.200	9.470
12	120	20 V	0.520	1.200	8.200	9.600

Table 2 Sensors technical characteristics.
Source: Own Elaboration

ISSN 2531-2960

	Sensor 1	Sensor 2	Sensor 3	Average
1	1686.000	1613.000	1412.000	1570.333
2	1709.000	1802.000	1440.000	1650.333
3	1686.000	1850.000	1450.000	1662.000
4	1700.000	1800.000	1500.000	1666.667
5	1730.000	1613.000	1498.000	1613.667
6	1500.000	1600.000	1300.000	1466.667
7	1600.000	1700.000	1400.000	1566.667
8	1630.000	1710.000	1450.000	1596.667
9	1660.000	1800.000	1500.000	1653.333
10	1686.000	1810.000	1800.000	1765.333
11	1700.000	1700.000	1800.000	1733.333
12	2200.000	1959.000	2080.000	2079.667

Table 3 Sensors technical characteristics.
Source: Own Elaboration

	Sensor 1	Sensor 2	Sensor 3	Average
1	1563.000	1654.000	1352.000	1523.000
2	1577.000	1600.000	1377.000	1518.000
3	1425.000	1529.730	1450.000	1468.243
4	1289.264	1477.860	1344.271	1370.465
5	950.000	850.000	1062.000	954.000
6	800.000	1000.000	950.000	916.667
7	1110.000	1097.000	924.000	1043.667
8	950.000	1000.000	1050.000	1000.000
9	786.000	850.000	926.000	854.000
10	922.000	930.000	1020.000	957.333
11	1250.000	1300.000	1200.000	1250.000
12	832.000	862.000	850.000	848.000

Table 4 Sensors technical characteristics.
Source: Own Elaboration

According with the experimental measurements tables, next figures show the behavior of DO, pH and turbidity.

Graphics 1-3 show the comparative values of initial and final DO for 10 V, 15 V and 20 V respectively during 30 min, 60 min, 90 min, and 120 min, and Graphics 4 shows the DO rate of change.

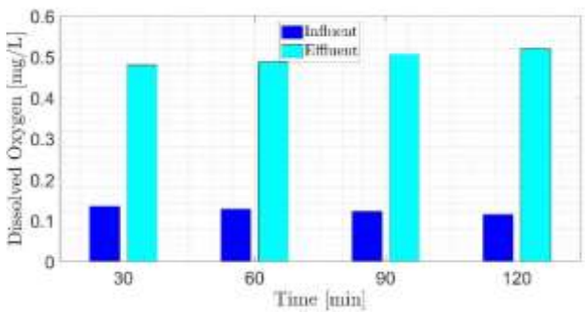

Graphic 1 Initial and final DO levels for 10 V.
Source: Own Elaboration

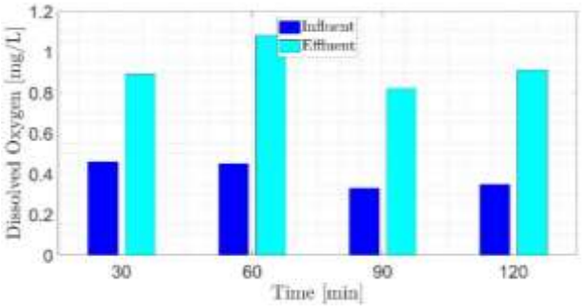

Graphic 2 Initial and final DO levels for 15 V.
Source: Own Elaboration

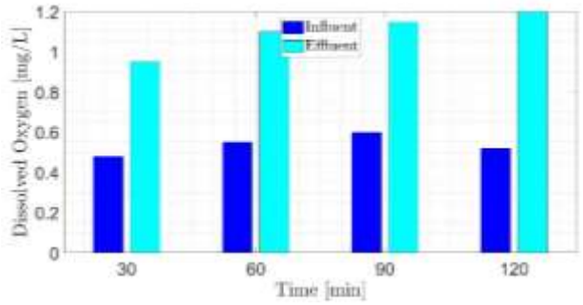

Graphic 3 Initial and final DO levels for 20 V.
Source: Own Elaboration

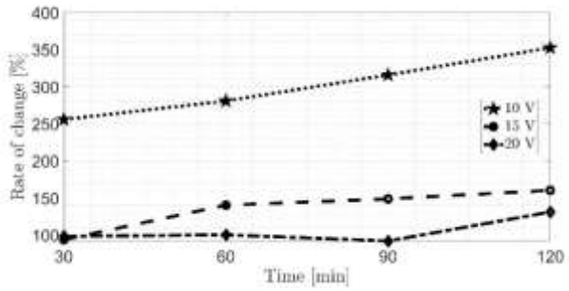

Graphic 4 DO rate of change
Source: Own Elaboration

From DO levels graphs, Graphics 5 and 6 show the behavior of dissolved oxygen in the effluent regarding to treatment time and applied voltage respectively.

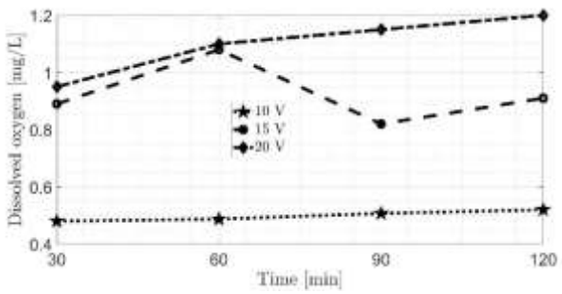

Graphic 5 DO variation in the effluent with respect to treatment time
Source: Own Elaboration

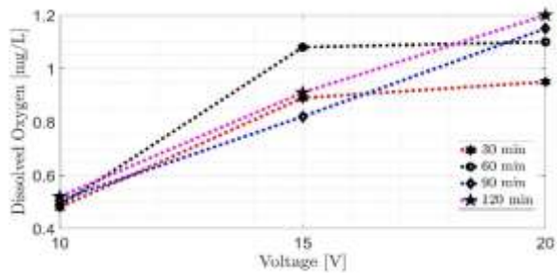

Graphic 6 DO variation in the effluent with respect to applied voltage
Source: Own Elaboration

Graphics 7-9 show the comparative values of initial and final pH for 10 V, 15 V and 20 V respectively during 30 min, 60 min, 90 min, and 120 min and Graphic 10 shows the pH rate of change. From the pH levels graphs, Graphics 11 and 12 show the behavior of pH in the effluent with respect to treatment time and applied voltage respectively.

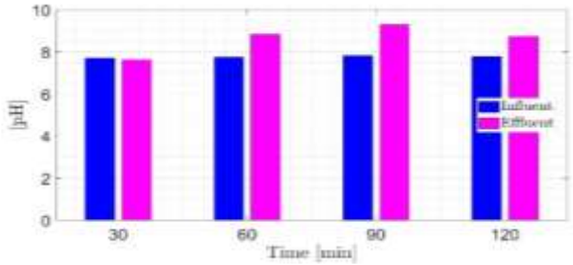

Graphic 7 Initial and final pH levels for 10 V
Source: Own Elaboration

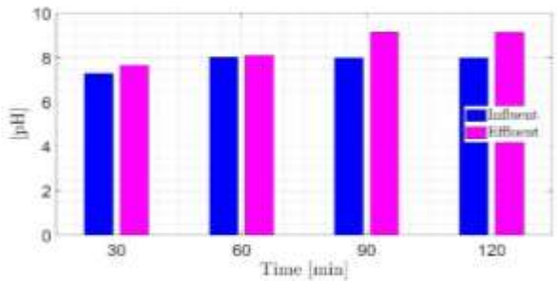

Graphic 8 Initial and final pH levels for 15 V.
Source: Own Elaboration

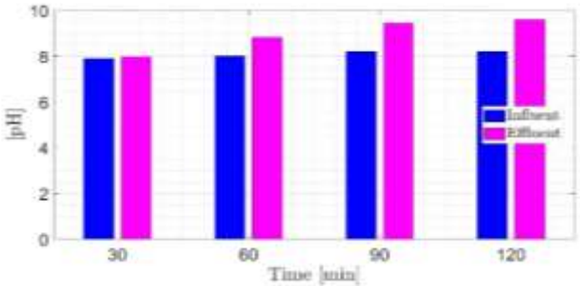

Graphic 9 Initial and final pH levels for 20 V.
Source: Own Elaboration

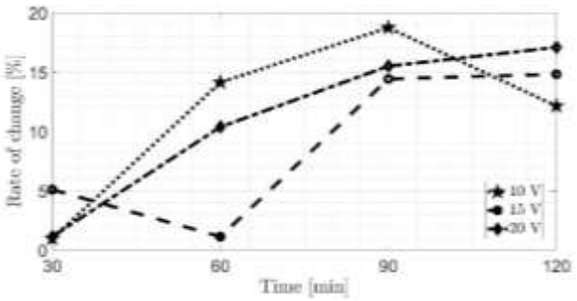

Graphic 10 pH rate of change
Source: Own Elaboration

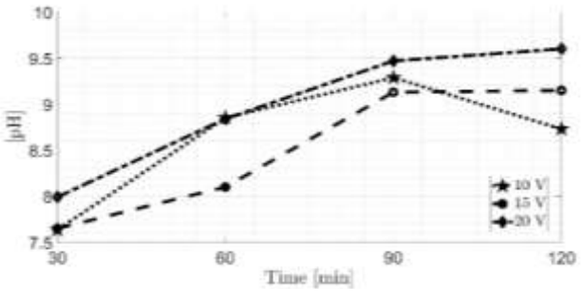

Grphic 11 pH variation in the effluent with respect to treatment time.
Source: Own Elaboration

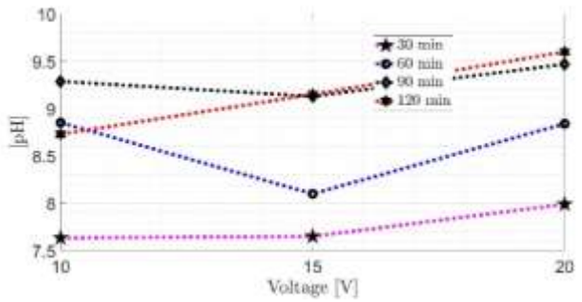

Graphic 12 pH variation in the effluent with respect to applied voltage
Source: Own Elaboration

Graphics 13-15 show the comparative values of initial and final turbidity for 10 V, 15 V and 20 V respectively during 30 min, 60 min, 90 min and 120 min, these graphs show the measurements of the three turbidity sensors and the average of them.

Also from the averages of the effluents, Figures 16, 17 and 18 show the turbidity rate of change, the behavior of turbidity in the effluent with respect to treatment time and applied voltage, respectively.

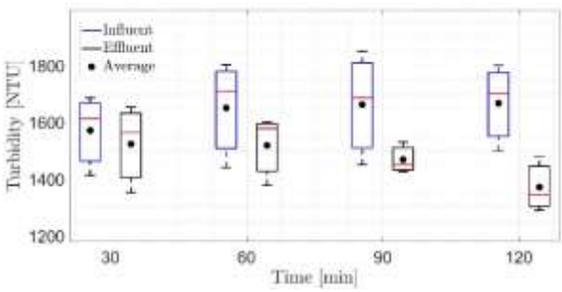

Graphic 13 Initial and final turbidity levels for 10 V
Source: Own Elaboration

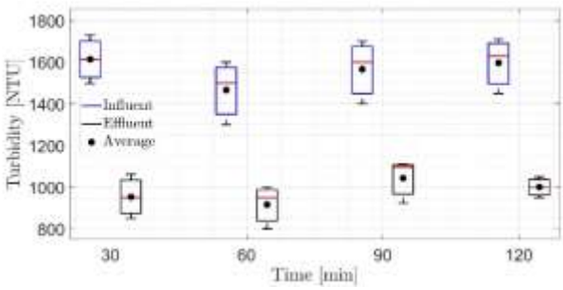

Graphic 14 Initial and final turbidity levels for 15 V.
Source: Own Elaboration

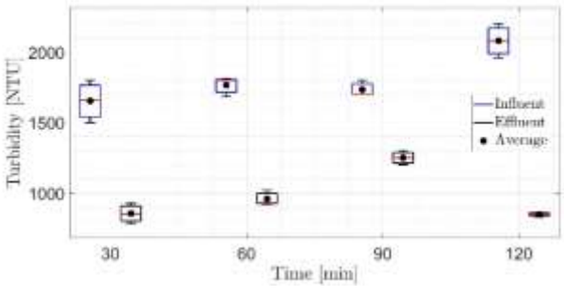

Graphic 15 Initial and final turbidity levels for 20 V.
Source: Own Elaboration

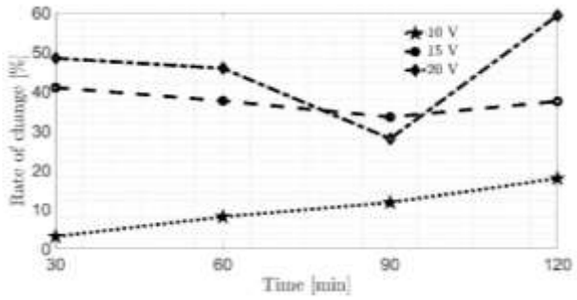

Graphic 16 Turbidity rate of change
Source: Own Elaboration

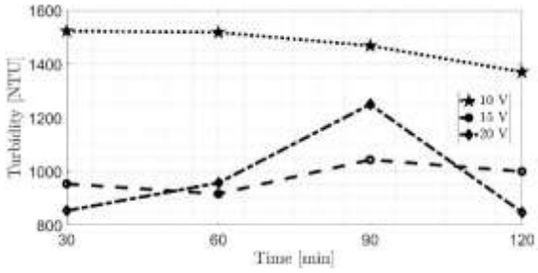

Graphic 17 Turbidity variation in the effluent with respect to treatment time
Source: Own Elaboration

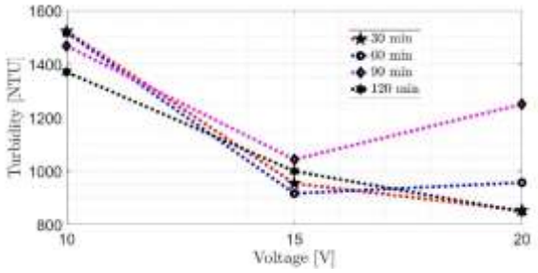

Graphic 18 Turbidity variation in the effluent with respect to applied voltage
Source: Own Elaboration

5 Conclusions

The measurement system allows online monitoring through the HMI of the variables dissolved oxygen, pH and turbidity in the influent and effluents of the grey water treatment process and determining changes of them quickly. Experimental tests of the treatment process were performed varying the applied voltage and duration of the EC process. The dissolve oxygen variable shows an increase when the applied voltage and treatment time are increased, and the pH variable also shows an increase when the applied voltage and treatment time are increased.

On the other hand the average turbidity measurements show a decrease when the applied voltage and treatment time are increased. Although the DO, pH and turbidity measurements in the influents show different values in all experiments, the highest percentage increase in DO was 352.20% in the experiment 4 with 10 V and 120 min of treatment, the pH had a maximum increase of 18.73% in the experiment 3 with 10 V and 90 min of treatment and the turbidity variable had a maximum decrease of 59.22% in the experiment 12 with 20 V and 120 min of treatment.

ISSN 2531-2960

Acknowledgements

This work was supported by IPN projects SIP 20196836 and SIP 20200191.

Referencias

[1] U. Nations, Water and sanitation - united nations sustainable, https://www.un.org/ sustainabledevelopment/water-and-sanitation/.

[2] M. Y. A. Mollah, R. Schennach, J. R. Parga, D. L. Cocke, Journal of hazardous materials 2001, 84, 1 29.

[3] G. Chen, Separation and purification Technology 2004, 38, 1 11.

[4] S. Piña, M. Dominguez, G. Ramirez, Revista Mexicana de Ingenier´ıa Qu´ımica 2011, 10, 2.

[5] C. E. B. Díaz, Aplicaciones electroqu´ımicas al tratamiento de aguas residuales, Reverte, 2014.

[6] S. Garcia-Segura, M. M. S. Eiband, J. V. de Melo, C. A. Martínez-Huitle, Journal of Electroanalytical Chemistry 2017, 801 267.

[7] S. Mondal, M. K. Purkait, S. De, Advances in dye removal technologies, Springer, 2018.

[8] R. Bastian, D. Murray, Guidelines for water reuse. us epa office of research and development, washington, dc, Technical report, EPA/600/R-12/618, 2012.

[9] N. O. Mexicana, Diario Oficial de la Federaci´on: Mexico City, Mexico 1997.

[10] P. K. Holt, G. W. Barton, C. A. Mitchell, Chemosphere 2005, 59, 3 355.

[11] S. Zhang, J. Zhang, W. Wang, F. Li, X. Cheng, Solar Energy Materials and Solar Cells 2013, 117 73.

[12] G. Sharma, J. Choi, H. Shon, S. Phuntsho, Desalination and water treatment 2011, 32, 1-3 381.

[13] D. Marmanis, K. Dermentzis, A. Christoforidis, K. Ouzounis, A. Moumtzakis, Desalination and Water Treatment 2015, 56, 11 2988.

[14] C. Nawarkar, V. Salkar, Fuel 2019, 237 222.

[15] M. M. Emamjomeh, M. Sivakumar, Journal of Environmental Management 2009, 90, 2 1204.

[16] M. M. Emamjomeh, M. Sivakumar, Journal of Environmental Management 2009, 90, 5 1663.

[17] DFRobot, Turbidity sensor sku sen0189, https://wiki.dfrobot.com/Turbidity_sensor_SKU_ _SEN0189#target_4.

[18] DFRobot, Gravity analog dissolved oxygen sensor sku sen0237, https://wiki.dfrobot.com/ Gravity__Analog_Dissolved_Oxygen_Sensor_ SKU_SEN0237.

[19] DFRobot, Industrial ph electrode sku fit0348, https://wiki.dfrobot.com/Industrial_pH_ electrode_SKU_FIT0348_.

[20] Arduino, Arduino mega 2560 rev3, https://store.arduino.cc/usa/mega-2560-r3.

[21] Y. Wei, Y. Jiao, D. An, D. Li, W. Li, Q. Wei, Sensors 2019, 19, 18 3995.

[22] C. E. Boyd, C. S. Tucker, R. Viriyatum, North American Journal of Aquaculture 2011, 73, 4 403.

[23] J. Essick, Hands-on introduction to LabVIEW for scientists and engineers, Oxford University Press, 2018.

[24] M. Michael, USA, O'Relly 2012.

[Title in Times New Roman and Bold No. 14 in English and Spanish]

Surname (IN UPPERCASE), Name 1st Author†*, Surname (IN UPPERCASE), Name 1st Coauthor, Surname (IN UPPERCASE), Name 2nd Coauthor and Surname (IN UPPERCASE), Name 3rd Coauthor

Institutional Affiliation of Author including Dependency (No.10 Times New Roman and Italic)

International Identification of Science - Technology and Innovation

ID 1st Author: (ORC ID - Researcher ID Thomson, arXiv Author ID - PubMed Author ID - Open ID) and CVU 1st author: (Scholar-PNPC or SNI-CONACYT) (No.10 Times New Roman)

ID 1st Coauthor: (ORC ID - Researcher ID Thomson, arXiv Author ID - PubMed Author ID - Open ID) and CVU 1st coauthor: (Scholar or SNI) (No.10 Times New Roman)

ID 2nd Coauthor: (ORC ID - Researcher ID Thomson, arXiv Author ID - PubMed Author ID - Open ID) and CVU 2nd coauthor: (Scholar or SNI) (No.10 Times New Roman)

ID 3rd Coauthor: (ORC ID - Researcher ID Thomson, arXiv Author ID - PubMed Author ID - Open ID) and CVU 3rd coauthor: (Scholar or SNI) (No.10 Times New Roman)

(Report Submission Date: Month, Day, and Year); Accepted (Insert date of Acceptance: Use Only ECORFAN)

Abstract (In English, 150-200 words)

Objectives
Methodology
Contribution

Abstract (In Spanish, 150-200 words)

Objectives
Methodology
Contribution

Keywords (In English)

Indicate 3 keywords in Times New Roman and Bold No. 10

Keywords (In Spanish)

Indicate 3 keywords in Times New Roman and Bold No. 10

Citation: Surname (IN UPPERCASE), Name 1st Author, Surname (IN UPPERCASE), Name 1st Coauthor, Surname (IN UPPERCASE), Name 2nd Coauthor and Surname (IN UPPERCASE), Name 3rd Coauthor. Paper Title. Journal of Technological Development. Year 1-1: 1-11 [Times New Roman No.10]

* Correspondence to Author (example@example.org)
† Researcher contributing as first author.

Introduction

Text in Times New Roman No.12, single space.

General explanation of the subject and explain why it is important.

What is your added value with respect to other techniques?

Clearly focus each of its features

Clearly explain the problem to be solved and the central hypothesis.

Explanation of sections Article.

Development of headings and subheadings of the article with subsequent numbers

[Title No.12 in Times New Roman, single spaced and bold]

Products in development No.12 Times New Roman, single spaced.

Including graphs, figures and tables-Editable

In the article content any graphic, table and figure should be editable formats that can change size, type and number of letter, for the purposes of edition, these must be high quality, not pixelated and should be noticeable even reducing image scale.

[Indicating the title at the bottom with No.10 and Times New Roman Bold]

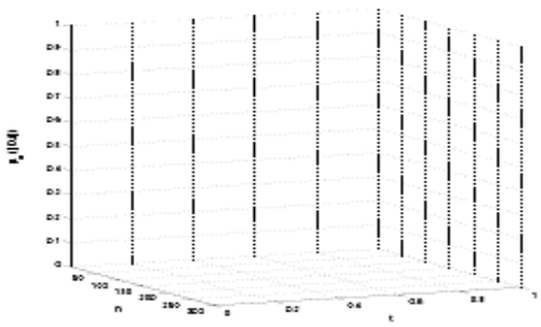

Graphic 1 Title and *Source (in italics)*

Should not be images-everything must be editable.

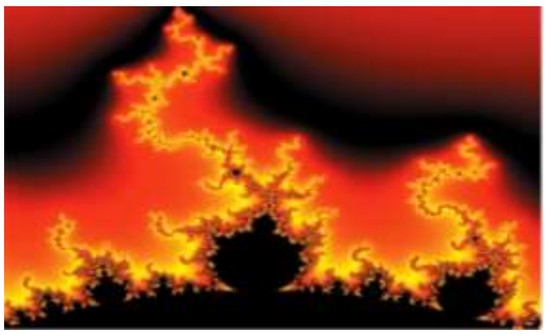

Figure 1 Title and *Source (in italics)*

Should not be images-everything must be editable.

Table 1 Title and *Source (in italics)*

Should not be images-everything must be editable.

Each article shall present separately in **3 folders**: a) Figures, b) Charts and c) Tables in .JPG format, indicating the number and sequential Bold Title.

For the use of equations, noted as follows:

$$Y_{ij} = \alpha + \sum_{h=1}^{r} \beta_h X_{hij} + u_j + e_{ij} \quad (1)$$

Must be editable and number aligned on the right side.

Methodology

Develop give the meaning of the variables in linear writing and important is the comparison of the used criteria.

Results

The results shall be by section of the article.

Annexes

Tables and adequate sources

Thanks

Indicate if they were financed by any institution, University or company.

ISSN: 2531-2960

Conclusions

Explain clearly the results and possibilities of improvement.

References

Use APA system. Should not be numbered, nor with bullets, however if necessary numbering will be because reference or mention is made somewhere in the Article.

Use Roman Alphabet, all references you have used must be in the Roman Alphabet, even if you have quoted an Article, book in any of the official languages of the United Nations (English, French, German, Chinese, Russian, Portuguese, Italian, Spanish, Arabic), you must write the reference in Roman script and not in any of the official languages.

Technical Specifications

Each article must submit your dates into a Word document (.docx):

Journal Name
Article title
Abstract
Keywords
Article sections, for example:

1. Introduction
2. Description of the method
3. Analysis from the regression demand curve
4. Results
5. Thanks
6. Conclusions
7. References

Author Name (s)
Email Correspondence to Author
References

Intellectual Property Requirements for editing:

-Authentic Signature in Color of Originality Format Author and Coauthors

-Authentic Signature in Color of the Acceptance Format of Author and Coauthors

ISSN: 2531-2960

Reservation to Editorial Policy

Journal of Technological Development reserves the right to make editorial changes required to adapt the Articles to the Editorial Policy of the Research Journal. Once the Article is accepted in its final version, the Research Journal will send the author the proofs for review. ECORFAN® will only accept the correction of errata and errors or omissions arising from the editing process of the Research Journal, reserving in full the copyrights and content dissemination. No deletions, substitutions or additions that alter the formation of the Article will be accepted.

Code of Ethics - Good Practices and Declaration of Solution to Editorial Conflicts

Declaration of Originality and unpublished character of the Article, of Authors, on the obtaining of data and interpretation of results, Acknowledgments, Conflict of interests, Assignment of rights and Distribution

The ECORFAN-Mexico, S.C Management claims to Authors of Articles that its content must be original, unpublished and of Scientific, Technological and Innovation content to be submitted for evaluation.

The Authors signing the Article must be the same that have contributed to its conception, realization and development, as well as obtaining the data, interpreting the results, drafting and reviewing it. The Corresponding Author of the proposed Article will request the form that follows.

Article title:

– The sending of an Article to Journal of Technological Development emanates the commitment of the author not to submit it simultaneously to the consideration of other series publications for it must complement the Format of Originality for its Article, unless it is rejected by the Arbitration Committee, it may be withdrawn.

– None of the data presented in this article has been plagiarized or invented. The original data are clearly distinguished from those already published. And it is known of the test in PLAGSCAN if a level of plagiarism is detected Positive will not proceed to arbitrate.

– References are cited on which the information contained in the Article is based, as well as theories and data from other previously published Articles.

– The authors sign the Format of Authorization for their Article to be disseminated by means that ECORFAN-Mexico, S.C. In its Holding Spain considers pertinent for disclosure and diffusion of its Article its Rights of Work.

– Consent has been obtained from those who have contributed unpublished data obtained through verbal or written communication, and such communication and Authorship are adequately identified.

– The Author and Co-Authors who sign this work have participated in its planning, design and execution, as well as in the interpretation of the results. They also critically reviewed the paper, approved its final version and agreed with its publication.

– No signature responsible for the work has been omitted and the criteria of Scientific Authorization are satisfied.

– The results of this Article have been interpreted objectively. Any results contrary to the point of view of those who sign are exposed and discussed in the Article.

Copyright and Access

The publication of this Article supposes the transfer of the copyright to ECORFAN-Mexico, SC in its Holding Spain for its Journal of Technological Development, which reserves the right to distribute on the Web the published version of the Article and the making available of the Article in This format supposes for its Authors the fulfilment of what is established in the Law of Science and Technology of the United Mexican States, regarding the obligation to allow access to the results of Scientific Research.

Article Title:

Name and Surnames of the Contact Author and the Coauthors	Signature
1.	
2.	
3.	
4.	

Principles of Ethics and Declaration of Solution to Editorial Conflicts

Editor Responsibilities

The Publisher undertakes to guarantee the confidentiality of the evaluation process, it may not disclose to the Arbitrators the identity of the Authors, nor may it reveal the identity of the Arbitrators at any time.

The Editor assumes the responsibility to properly inform the Author of the stage of the editorial process in which the text is sent, as well as the resolutions of Double-Blind Review.

The Editor should evaluate manuscripts and their intellectual content without distinction of race, gender, sexual orientation, religious beliefs, ethnicity, nationality, or the political philosophy of the Authors.

The Editor and his editing team of ECORFAN® Holdings will not disclose any information about Articles submitted to anyone other than the corresponding Author.

The Editor should make fair and impartial decisions and ensure a fair Double-Blind Review.

Responsibilities of the Editorial Board

The description of the peer review processes is made known by the Editorial Board in order that the Authors know what the evaluation criteria are and will always be willing to justify any controversy in the evaluation process. In case of Plagiarism Detection to the Article the Committee notifies the Authors for Violation to the Right of Scientific, Technological and Innovation Authorization.

Responsibilities of the Arbitration Committee

The Arbitrators undertake to notify about any unethical conduct by the Authors and to indicate all the information that may be reason to reject the publication of the Articles. In addition, they must undertake to keep confidential information related to the Articles they evaluate.

Any manuscript received for your arbitration must be treated as confidential, should not be displayed or discussed with other experts, except with the permission of the Editor.

The Arbitrators must be conducted objectively, any personal criticism of the Author is inappropriate.

The Arbitrators must express their points of view with clarity and with valid arguments that contribute to the Scientific, Technological and Innovation of the Author.

The Arbitrators should not evaluate manuscripts in which they have conflicts of interest and have been notified to the Editor before submitting the Article for Double-Blind Review.

Responsibilities of the Authors

Authors must guarantee that their articles are the product of their original work and that the data has been obtained ethically.

Authors must ensure that they have not been previously published or that they are not considered in another serial publication.

Authors must strictly follow the rules for the publication of Defined Articles by the Editorial Board.

The authors have requested that the text in all its forms be an unethical editorial behavior and is unacceptable, consequently, any manuscript that incurs in plagiarism is eliminated and not considered for publication.

Authors should cite publications that have been influential in the nature of the Article submitted to arbitration.

Information services

Indexation - Bases and Repositories

RESEARCH GATE (Germany)
GOOGLE SCHOLAR (Citation indices-Google)
MENDELEY (Bibliographic References Manager)
REDIB (Ibero-American Network of Innovation and Scientific Knowledge- CSIC)
HISPANA (Information and Bibliographic Orientation-Spain)

Publishing Services

Citation and Index Identification H
Management of Originality Format and Authorization
Testing Article with PLAGSCAN
Article Evaluation
Certificate of Double-Blind Review
Article Edition
Web layout
Indexing and Repository
ArticleTranslation
Article Publication
Certificate of Article
Service Billing

Editorial Policy and Management

38 Matacerquillas, CP-28411. Moralzarzal –Madrid-España. Phones: +52 1 55 6159 2296, +52 1 55 1260 0355, +52 1 55 6034 9181; Email: contact@ecorfan.org www.ecorfan.org

Journal of Technological Development

2 5 3 1 2 9 6 0
ISSN 2531 - 2960

www.ecorfan.org